

NATIONAL ADVISORY COMMITTEE FOR AERONAUTICS

# WARTIME REPORT

ORIGINALLY ISSUED  
August 1941 as  
Memorandum Report

POWER-ON WIND-TUNNEL TESTS OF THE 1/8-SCALE

MODEL OF THE BREWSTER F2A AIRPLANE WITH

FULL-SPAN SLOTTED FLAPS

By John G. Lowry

Langley Memorial Aeronautical Laboratory  
Langley Field, Va.

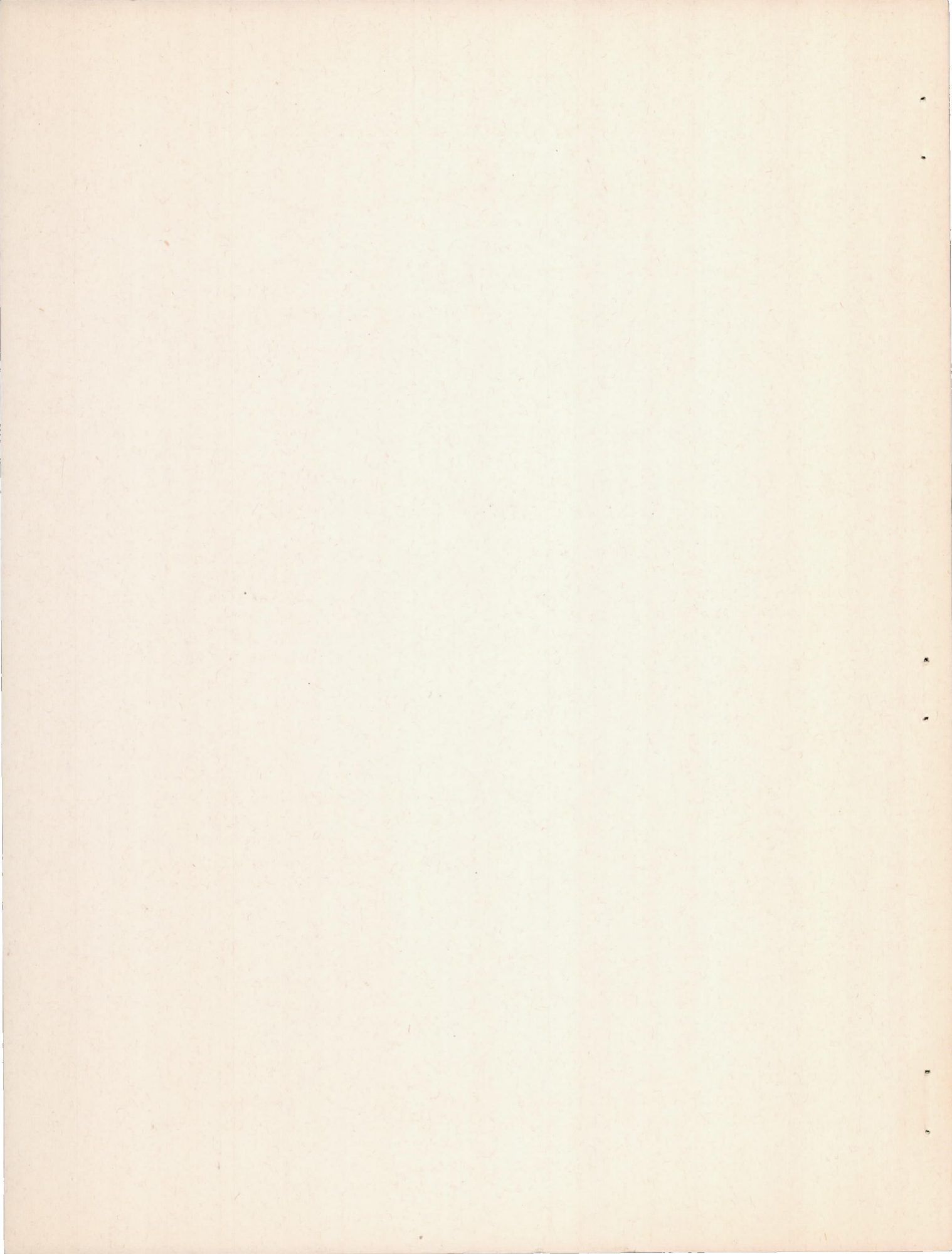
**FILE COPY**

To be returned to  
the files of the National  
Advisory Committee  
for Aeronautics  
Washington, D. C.



WASHINGTON

NACA WARTIME REPORTS are reprints of papers originally issued to provide rapid distribution of advance research results to an authorized group requiring them for the war effort. They were previously held under a security status but are now unclassified. Some of these reports were not technically edited. All have been reproduced without change in order to expedite general distribution.



NATIONAL ADVISORY COMMITTEE FOR AERONAUTICS

MEMORANDUM REPORT

for the

Bureau of Aeronautics, Navy Department

POWER-ON WIND-TUNNEL TESTS OF THE 1/8-SCALE

MODEL OF THE BREWSTER F2A AIRPLANE WITH

FULL-SPAN SLOTTED FLAPS

By John G. Lowry

INTRODUCTION

At the request of the Bureau of Aeronautics, Navy Department, tests were made in the 7- by 10-foot wind tunnel of the 1/8-scale model of the Brewster F2A airplane with full-span slotted flaps. The object of the tests was to determine the power-on static lateral and longitudinal stability of the complete model with a new wing which had a full-span slotted flap and a plain and slot-lip aileron for lateral control.

MODEL

The 1/8-scale model of the Brewster F2A airplane was furnished by the Brewster Aeronautical Corporation and no attempt was made to check its dimensions. A three-view drawing of the complete model with the original wing is shown in figure 1 and of the modified wing in figure 2. The modified wing which has a full-span NACA slotted flap was used in this series of tests.

The angle of attack of the reference thrust line was determined by means of leveling lugs that were fitted into holes previously drilled in the fuselage. The stabilizer, elevator, rudder, flap, and aileron angles were set by means of templates furnished with the model.

Power for the model was obtained from a 35-horsepower water-cooled induction motor that was mounted within the fuselage contour. This motor, designed especially for power-on model tests, has an alternator tachometer built into it to measure the rpm of the

propeller. Power and water leads were run into the model through a streamlined fairing which covered both the leads and the model support strut.

The propeller used in these tests had a diameter 6 percent larger than the scale size for the prototype and was probably not geometrically similar to the prototype propeller since it consisted of blades available at the 7- by 10-foot wind tunnel. The blades were mounted in an especially designed six-blade hub and the three-blade propeller was made by assembling three blades in the hub.

### TESTS AND RESULTS

Test conditions.- The tests were made in the NACA 7- by 10-foot wind tunnel. All the tests, except as noted below, were run at a dynamic pressure of 16.37 pounds per square foot which corresponds to a velocity of about 80 miles per hour under standard sea-level conditions, and to a test Reynolds number of about 570,000 based on the mean aerodynamic chord of 9.36 inches. The effective Reynolds number,  $R_e$ , was 912,000 based on a turbulence factor for the 7- by 10-foot tunnel of 1.6.

Coefficients.- The results of the tests are given in the form of standard NACA coefficients of forces and moments based on model wing area, wing span, and mean aerodynamic chord. All moments are taken about the center-of-gravity location of the complete airplane shown on figure 1 (normal fighter, landing gear retracted). The data are referred to the stability axes, a system in which the X axis is the intersection of the plane of symmetry of the airplane with a plane perpendicular to the plane of symmetry and parallel with the relative wind direction, the Y axis is perpendicular to the plane of symmetry, and the Z axis is in the plane of symmetry and perpendicular to the X axis. The coefficients are defined as follows:

$$C_D \quad \text{drag coefficient (propellers removed)} = \frac{X}{qS}$$

$$C_{DR} \quad \text{resultant-drag coefficient} = \frac{X}{qS}$$

$$C_Y \quad \text{lateral-force coefficient} = \frac{Y}{qS}$$

$$C_L \quad \text{lift coefficient} = \frac{L}{qS}$$

$$C_l \quad \text{rolling-moment coefficient about c.g.} = \frac{l}{qSb}$$

$C_m$  pitching-moment coefficient about c.g. =  $\frac{m}{qSc}$

$C_n$  yawing-moment coefficient about c.g. =  $\frac{n}{qSb}$

where

- X force along X axis; positive when directed backwards
- Y force along Y axis; positive when directed to right
- L force along Z axis; positive when directed upwards
- $l$  rolling moment about X axis; positive when it tends to depress the right wing
- $m$  pitching moment about Y axis; positive when it tends to depress the tail
- $n$  yawing moment about Z axis; positive when it tends to retard right wing
- $q$  dynamic pressure =  $\frac{1}{2}\rho V^2$  (16.37 pounds per square foot)
- S wing area (3.265 square feet)
- $c$  mean aerodynamic chord (0.78 foot)
- $b$  wing span (4.38 feet)

The following propeller coefficients are used:

- $T_c'$  effective model-thrust coefficient =  $\frac{T}{qS}$
- $T_c$  effective propeller-thrust coefficient =  $\frac{T}{\rho V^2 D^2}$
- $V/nD$  advance diameter ratio

where

- T effective thrust in pounds
- $\rho$  mass density of air in slugs per cubic foot
- V airspeed in feet per second
- D propeller diameter (1.36 feet)

n propeller speed in revolutions per second  
rpm propeller speed in revolutions per minute

Symbols. - Certain symbols are used in the text and figures, and are defined as follows:

$\alpha$  angle of attack of thrust line, degrees  
 $\psi$  angle of yaw, degrees; positive when nose of model moves to right  
 $i_T$  angle of stabilizer setting with respect to thrust line, degrees; positive with trailing edge down  
 $\delta_e$  elevator deflection (with respect to stabilizer chord), degrees; positive when trailing edge of elevator is moved down  
 $\delta_r$  rudder deflection, degrees; positive when trailing edge of rudder is moved to left  
 $\delta_f$  flap deflection, degrees; positive when trailing edge of flap is moved down  
 $\delta_a$  aileron deflection, degrees; positive when trailing edge of aileron is moved down (subscripts R and L denote right and left ailerons)  
 $\beta$  angle of propeller-blade setting measured at the 75 percent radius

Corrections. - The results have not been corrected for tares caused by the model support.

All the angles of attack, the drag coefficients, and the pitching-moment coefficients have been corrected for the effects of the tunnel walls. The jet-boundary corrections applied were computed as follows:

$$\text{Induced drag correction, } \Delta C_{D_i} = \delta \frac{S}{C} C_L^2 \quad (1)$$

$$\text{Induced angle-of-attack correction, } \Delta \alpha_1^{\circ} = \delta \frac{S}{C} C_L (57.3) \quad (2)$$

Pitching-moment-coefficient correction

$$\Delta C_m = \delta_{a_w} \frac{S}{C} \frac{dC_m}{di_T} C_L (57.3) \quad (3)$$

All corrections are added to tunnel data. In the aforementioned equations:

$$\delta = 0.115$$

$$\delta_{a_w} = 0.065$$

$$C = \text{tunnel cross-sectional area (69.59 square feet)}$$

$\frac{dC_m}{d\tau}$  = change in pitching-moment coefficient per degree change in stabilizer setting (This slope was furnished by contractor from New York University power-off data.)

No jet-boundary corrections were applied to the yawing- and rolling-moment coefficients. The corrections to the rolling- and yawing-moment coefficient are negligible for the size of the model used.

Test procedure.- Propeller calibrations were first made. They consisted of resultant-drag readings at various propeller speeds for several blade angles and for both the three- and six-blade propellers. The thrust coefficients were then computed from the equation:

$$T_c' = C_D - C_{D_R}$$

These propeller characteristics are presented in figure 3. Having these data, it was only necessary to vary the propeller speed to obtain the desired thrust assuming that the thrust was independent of angle of inclination of propeller. The effective thrust coefficients at which the tests were made are shown in figure 3-a. These curves were furnished by Mr. Michel, Brewster representative. It should be noted that these curves indicate the thrust for constant power for the prototype airplane over the speed range. The curves, therefore, represent climbing, diving, or accelerated conditions, and there is only one point on each curve that corresponds to steady level flight.

In making pitch tests, the rpm for each lift coefficient was determined from figures 3 and 3-a. The rpm was set and the angle of attack varied until the proper lift coefficient was obtained. After the first few runs it was possible to obtain an rpm versus angle of attack chart for a given model and power condition. All succeeding pitch tests were run in this manner.

The yaw tests were run at constant value of rpm. From the results of the pitch tests and the curves 3 and 3-a the correct rpm for a given angle of attack was obtained for the zero yaw condition. This value was then maintained throughout the yaw range.

For convenience in locating results, a résumé of the tests is given in the following table:

Test No.	Power Condition	No. Prop blades	$\beta$	$\delta_r$	$\delta_e$	$\delta_r$		Type Test	Figure
1	-----	3	20,30	0	0	0	$\alpha = \psi = 0$	Thrust Calib	3
2	Rated	3	30	0	0	0	$\psi = 0$	Pitch	4, 6
3	do	3	30	0	0	0	$\alpha \approx 2.5^\circ$	Yaw	13
4	do	3	30	0	0	0	$\alpha \approx 10^\circ$	do	5, 15
5	do	3	20	0	0	0	do	do	5
6	do	3	30	0	0	-15	do	do	15
7	$\frac{1}{2}$ Rated	3	30	0	0	0	$\psi = 0$	Pitch	6
8	Windmilling	3	30	0	0	0	do	do	6
9	Take-off	3	30	40	0	0	do	do	7
10	Windmilling	3	30	40	0	0	do	do	7
11	$\frac{1}{2}$ Rated	3	30	40	0	-15	$\alpha = 11\frac{1}{4}^\circ$	Yaw	16
12	do	3	30	40	0	0	do	do	12, 16
13	Windmilling	3	30	40	0	0	do	do	12
14	-----	6	30	0	0	0	$\psi = \alpha = 0$	Thrust Calib	3
15	Rated	6	30	0	0	0	$\psi = 0$	Pitch	4, 8
16	do	6	30	0	+2	0	do	do	8
17	do	6	30	0	-2	0	do	do	8
18	do	6	30	0	-4	0	do	do	8
20	do	3	30	40	0	0	do	do	7
20-a	$\frac{1}{2}$ Rated	3	30	40	0	0	do	do	7, 9
21-a	do	3	30	40	+2	0	do	do	9
22-a	do	3	30	40	-2	0	do	do	9
24	Take-off	3	30	40	0	0	$\alpha \approx -1.76^\circ$	Yaw	14
26	Rated	6	30	0	0	0	$\alpha \approx 10$	do	5

## DISCUSSION

Blade angle and number of blades.- The effect of the number of propeller blades and propeller-blade angle on the aerodynamic characteristics of the model are shown in figures 4 and 5. The curves are of value in interpolation of the results to actual conditions to be encountered on the prototype airplane which could not be exactly represented on the model. The effect of slipstream rotation as indicated by these curves is mainly on the trim condition and not on the stability of the model.

Longitudinal stability and control.- The effect of the addition of the propeller to the model and the application of various amounts of power is shown in figure 6 for the model with the flaps retracted and in figure 7 for the model with the flaps deflected  $40^\circ$  and the landing gear extended. With the clean model, flaps retracted, there is no apparent change in slope of pitching-moment curve with the addition of the windmilling propeller, but with the flaps deflected there is a slight decrease in the slope. While no attempt was made to duplicate the idling characteristics of the prototype engine-propeller installation, the present results are believed to be applicable.

The application of power decreases the slope of the pitching-moment coefficient curves progressively as the power is increased. For the clean model the application of rated power decreases the slope of the pitching-moment coefficient curve to the condition of neutral stability at the high-speed attitude. With flaps deflected the application of rated power decreases the slope of the pitching-moment-coefficient curve,  $dC_m/dC_L$ , from about  $-0.114$  for no power, no propeller, to about  $-0.015$  for rated power at a  $C_L$  of about  $0.9$ . These data indicate that the application of full-span flaps to the model does not result in longitudinal instability of the model with power.

The addition of the windmilling propeller had the expected effect on the resultant-drag coefficient, that is, the drag was increased over the values for the propeller-off condition. This value, however, will vary with changes in blade angle, decreasing as the blade angle is increased.

The addition of the windmilling propeller had a negligible effect on the slope of the lift-coefficient curve, but gave an apparent decrease in angle of attack for a given lift coefficient of  $0.5^\circ$  for clean model and of  $2^\circ$  to  $3^\circ$  with flaps deflected. For both conditions of the model, the windmilling propeller gave an increase

in maximum lift coefficient of approximately 0.25 which was accompanied, in the flap-neutral condition, by an increase of  $3^\circ$  in angle of attack for maximum lift. The addition of power increases the slope of the lift-coefficient curve as the power is increased. Sufficient power was not available to obtain maximum lift coefficients for the various power conditions, but previous tests have shown an increase in maximum lift coefficient with an increase in power.

The effect of small elevator deflections is shown in figure 8 for the model with flaps neutral and in figure 9 for the model with flaps deflected. The slight variation in resultant-drag coefficient in figure 8 between tests 15 and 16 and tests 17 and 18 may be the result of a slight variation in the blade angle as the propeller was disassembled between these two series of runs; however, the effect of pitching moment is expected to be small. The pitching-moment coefficient curves show no indication of tail stall in the lift range tested.

The elevator angles for trim are given in figure 10 for the clean model and in figure 11 for the model with flaps deflected. The elevator deflections for trim in figure 10 were obtained by interpolation of the pitching-moment data in figure 8 and the values of  $\delta_e$  in figure 11 were determined from extrapolation of the pitching-moment data of figure 9. These curves indicate that the clean model with rated power requires  $2^\circ$  down elevator to trim in the high-speed attitude while the model with flap deflected and half-rated power requires about  $7^\circ$  up elevator to trim at relatively high-lift coefficients.

An analysis made at the Laboratory indicates the possibility that the elevator hinge moments may be so large that the pilot will have difficulty handling the airplane in the flap-deflected high-speed condition because of the large up-elevator deflections required to trim the airplane. In addition, because of the large downwash angle at the tail associated with flap deflection, the elevator probably tends to float down which means a relatively large movement of the elevator from the position of zero hinge moment. Additional tests to determine the angle of attack of the tail with flaps down and half-rated power will be made in the 7- by 10-foot wind tunnel as soon as the 35-horsepower motor is available for tests. In addition, tests will be made with large elevator deflections to determine the elevator deflections for trim with the flap down. It is not considered good practice to extrapolate for the trim elevator angle as was done for preparation of figure 11 because of the pronounced effect of the elevator deflection on the longitudinal stability of powered models as shown in figure 8.

Lateral stability. - The effect of angle of attack, flap deflection, and power on the aerodynamic characteristics in yaw of the model

is given in figures 12 to 14 and the effect of rudder deflection is given in figures 15 and 16 for the clean model and model with flap deflected and landing gear extended.

The addition of power to the model with windmilling propeller and flap deflected, figure 12 changed the slope of the rolling-moment-coefficient curve,  $dC_l/d\psi$ , from 0.0013 for propeller windmilling to -0.0005 for half-rated power. The effective dihedral for the clean model in both the high-speed and high angle-of-attack condition is satisfactory; however, there is a decrease in slope of rolling-moment-coefficient curve with angle of attack (figs. 13 and 15). A comparison of the rolling-moment-coefficient curves of figures 14 and 15 shows that obtaining a given lift coefficient by deflecting the flaps decreases the slope of the rolling-moment-coefficient curve more than obtaining the same lift coefficient by increasing the angle of attack. There is, however, a slight increase in power in the flap-deflected condition but it is believed this slight increase does not affect the slope of the curve to any great extent.

The rolling-moment instability indicated with power and flaps deflected has been observed on all powered models tested in the 7- by 10-foot wind tunnel of airplanes with very low power loadings. It has also been observed in flight and it indicates inability to "pick up" a wing with the rudder when flying with flaps down at moderate or large thrust coefficients.

The addition of power to the model with flaps deflected shifted the trim angle in yaw from  $-1.5^\circ$  for propeller windmilling to  $-16^\circ$  for half power and also increased the slope of the yawing-moment-coefficient curve. The increase in power also increased the slope of the lateral-force coefficient curve (fig. 12).

The deflection of the rudder has no effect on the slope of the rolling- or yawing-moment-coefficient curves but shifts the trim angle  $\frac{1}{2}^\circ$  per degree of rudder deflection for the flap neutral condition and  $1^\circ$  per degree of rudder deflection for the flap deflected condition. Thus, it would require about  $15^\circ$  rudder to trim the model with flaps deflected but only about  $9^\circ$  rudder with the flaps neutral. The vertical tail shows indication of stall at about  $30^\circ$  yaw for both model conditions. Since no attempt was made to represent exactly the slipstream rotation of the prototype airplane in the model tests the actual rudder deflections may be different on the airplane from those shown for the model. Tests of the powered models have indicated that rudder deflections for trim are best determined when the model and prototype propellers are operating at the same thrust-torque ratio.

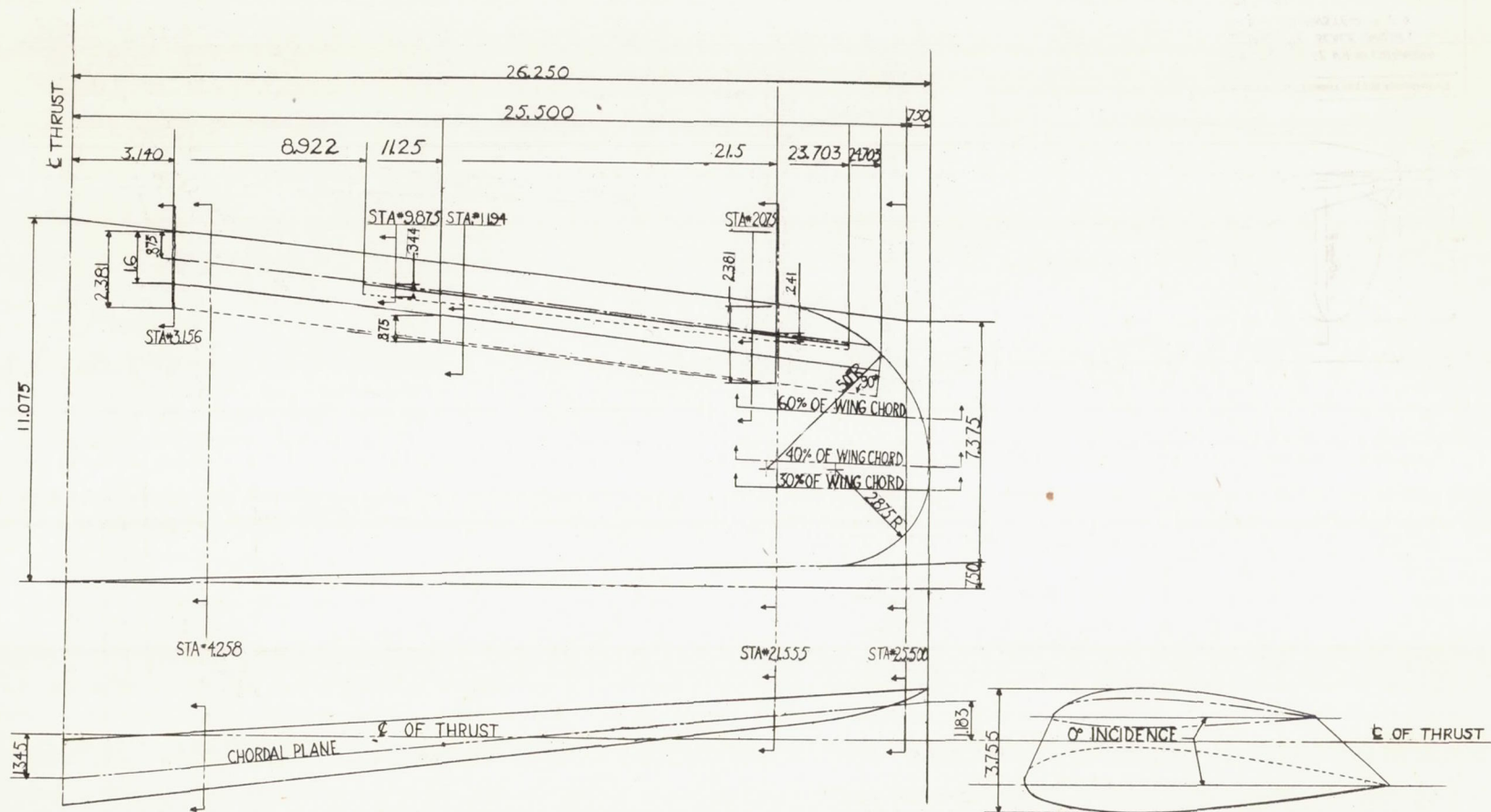
No aileron tests were made with the powered model since it is believed that the data presented in reference 1 without power are applicable.

Langley Memorial Aeronautical Laboratory,  
National Advisory Committee for Aeronautics,  
Langley Field, Va., August 21, 1941.

REFERENCE

1. Lowry, John G.: Power-Off Wind-Tunnel Tests of the 1/8-Scale Model of the Brewster F2A Airplane. NACA MR, June 21, 1941.





NATIONAL ADVISORY  
COMMITTEE FOR AERONAUTICS

Figure 2. - Three view drawing modified wing for  $\frac{1}{8}$ -scale model Brewster F2A airplane.

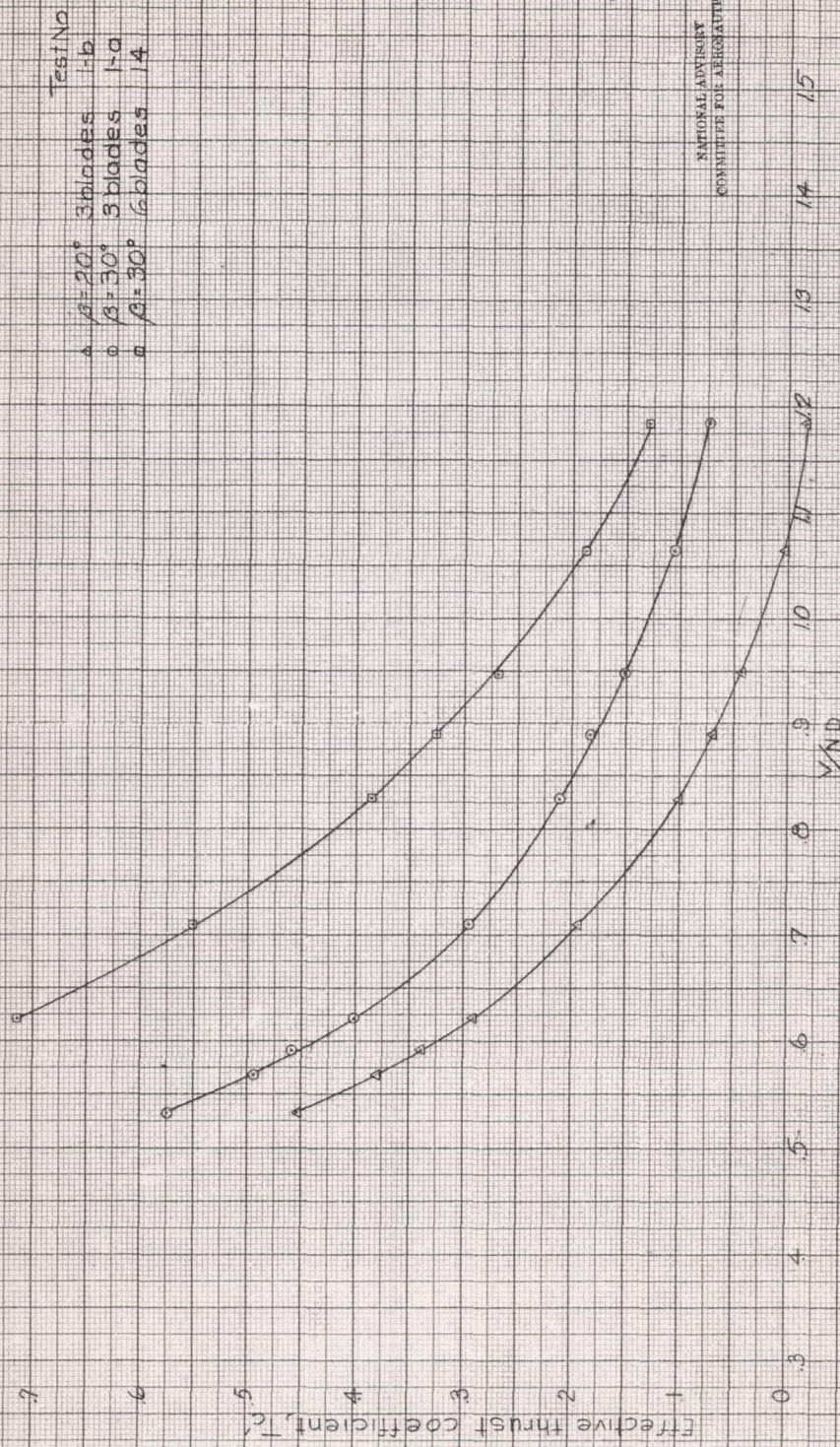


FIGURE 3-Effective Thrust coefficient calibration of the propellers of the 1/8 scale model of the Brewster F 2A airplane.  $\alpha = 0$   $\psi = 0$   $\delta = 0$   $r = 0$   $\beta = 20^\circ$ ,  $\beta = 30^\circ$ , landing gear retracted.

5-20-41

FIGURE 3d. - THRUST COEFFICIENT  $T_c - \rho V^2 D^2 = \frac{G}{(V_{IND})^2}$   
 FOR  
 BREWSTER F2A TYPE AIRPLANE

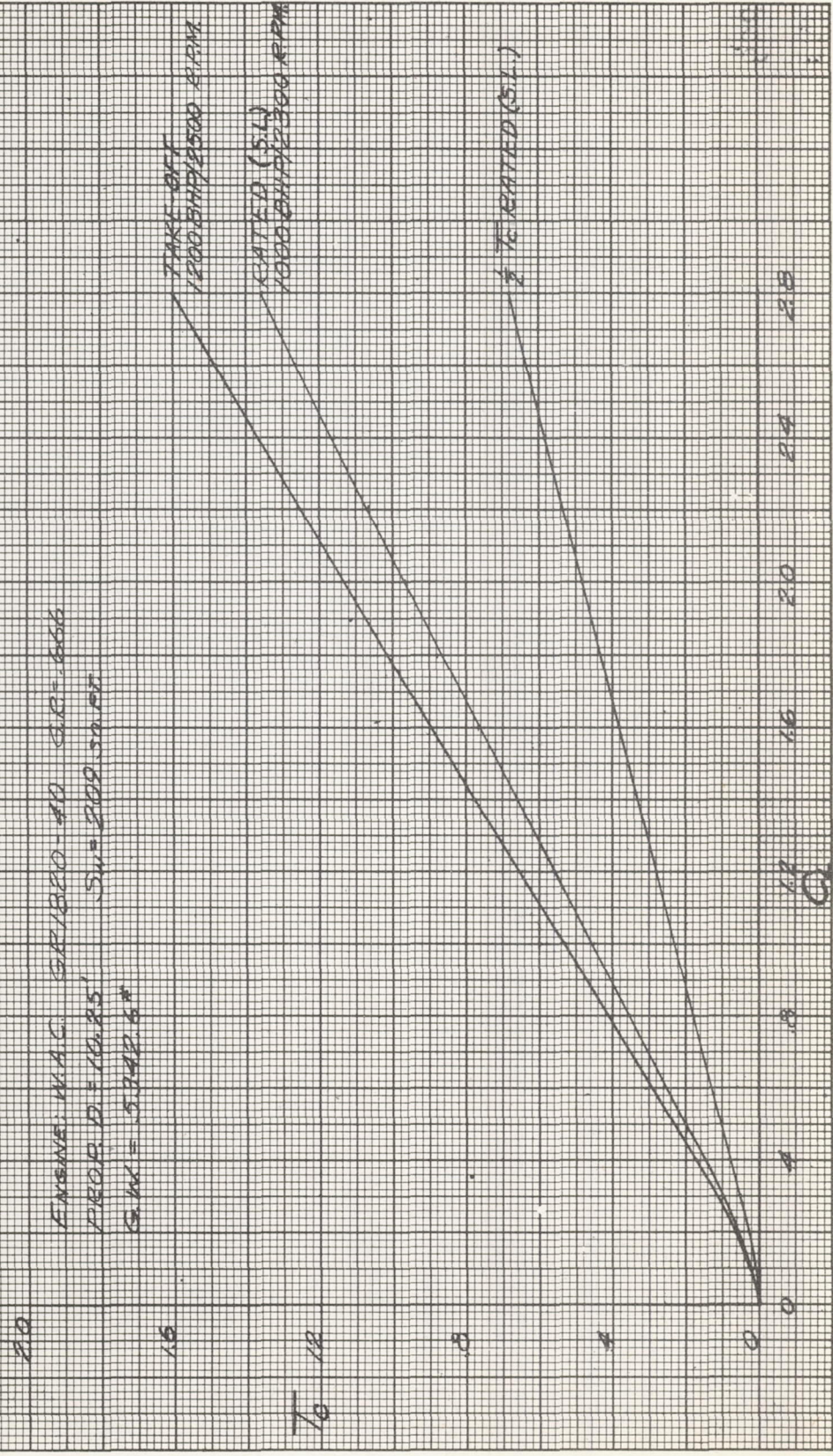
NATIONAL BUREAU OF  
 AERONAUTICS  
 COMPUTER FOR AERONAUTICS

ENGINE: WAC GR1820-40 CR-666  
 PROP. D = 10.25' S.W. = 200.50 HP  
 G.W. = 5342.6#

TAKE-OFF  
 1200 RPM/2500 RPM

CATL D (S.L.)  
 1000 RPM/2300 RPM

$\frac{1}{2}$  T.C. RATED (S.L.)



2.8  
2.4  
2.0  
1.6  
1.2  
0.8  
0.4  
0

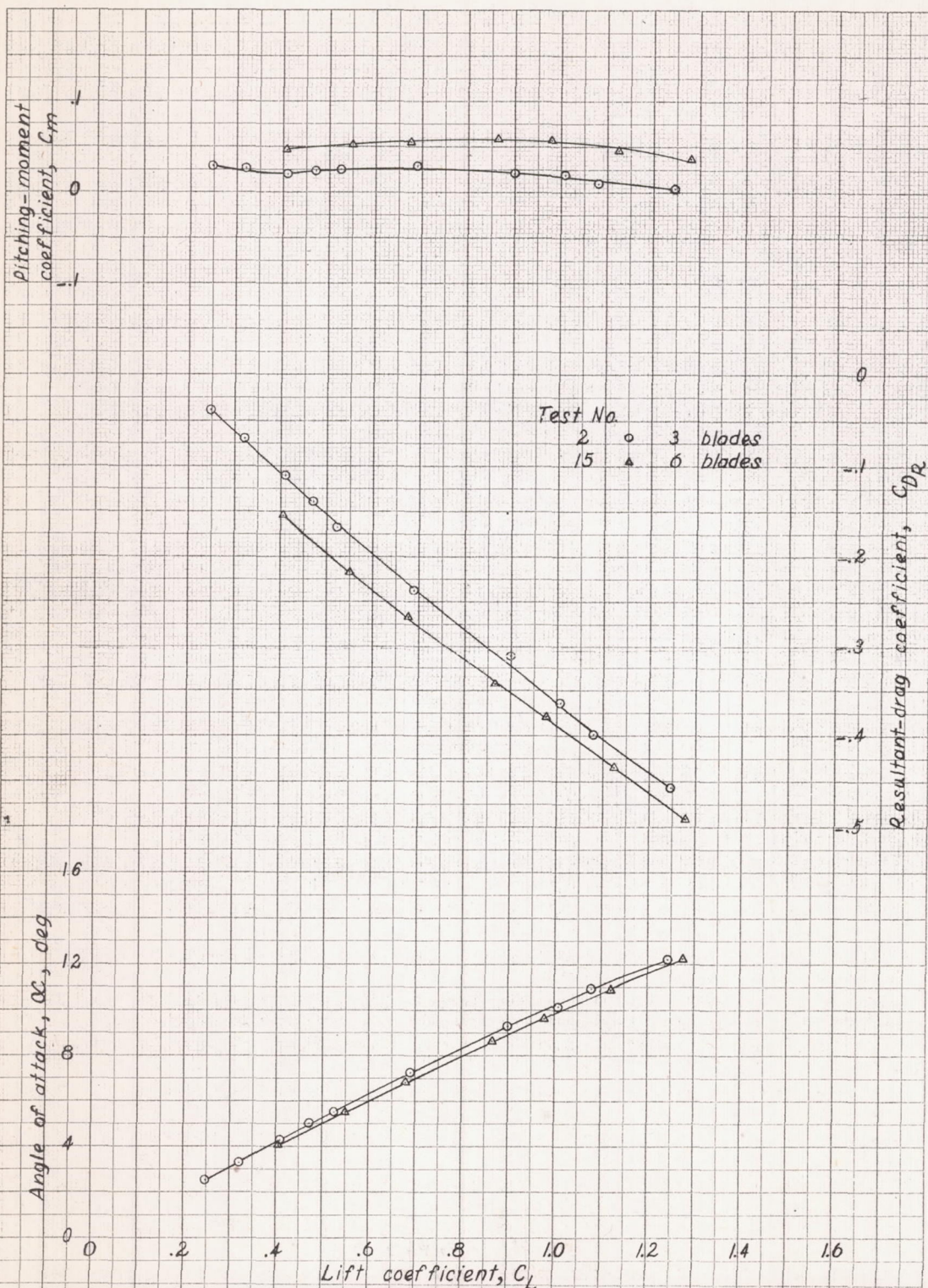


Figure 4.- Effect of number of propeller blades on the aerodynamic characteristics of the 1/8 scale model of the Brewster F2A airplane. Approximately rated power.  $\psi = \delta_f = \delta_a = \delta_r = \delta_e = 0$ ,  $i_t = -0.9$ , landing gear retracted.  $\beta = 30^\circ$ ,  $q = 16.37$  lbs/ft<sup>2</sup>.

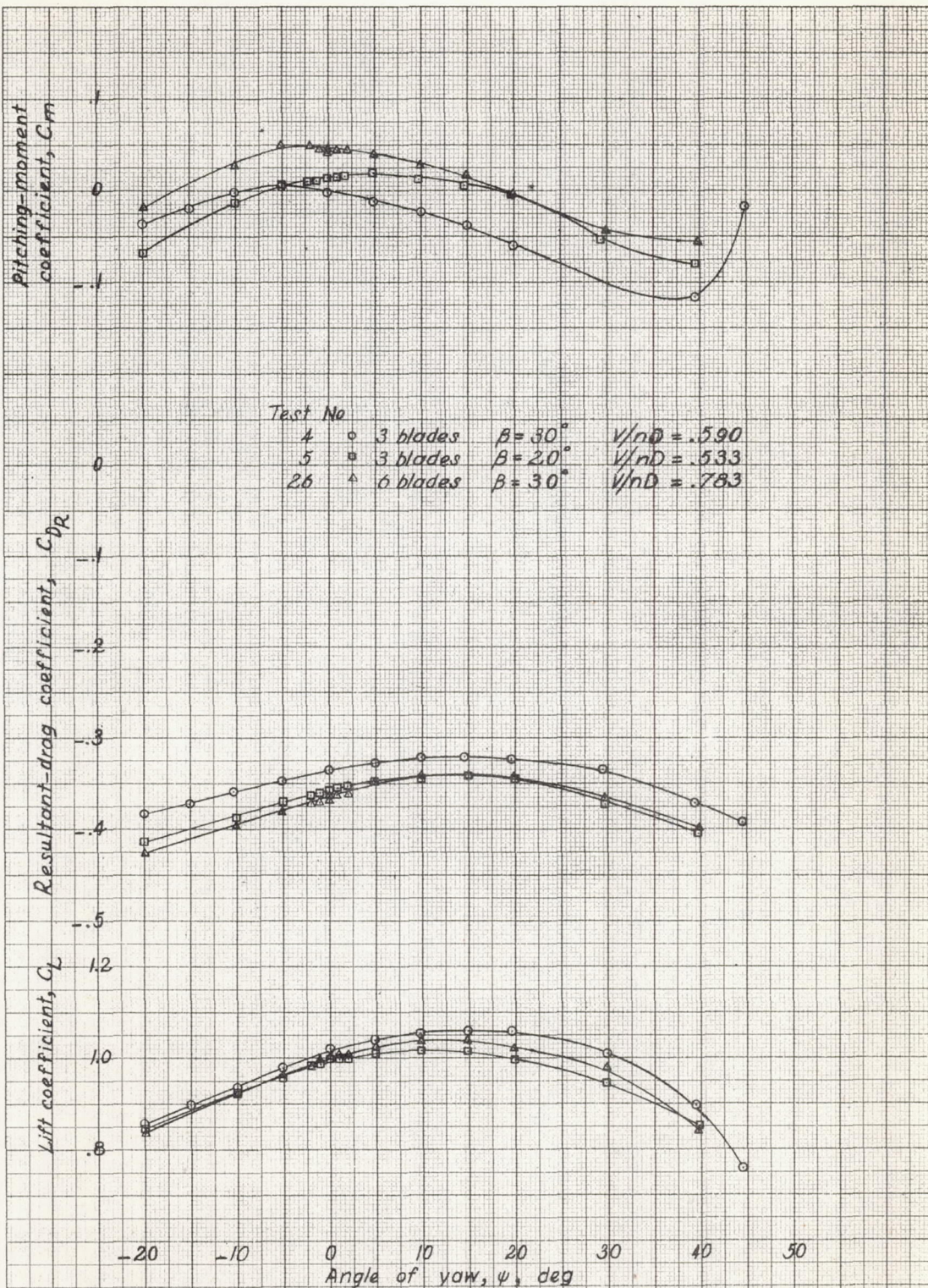


Figure 5.-Effect of propeller blade angle and number of blades on the aerodynamic characteristics in yaw of the  $\sqrt{3}$  scale model of the Brewster F2A airplane. Approximately rated power. Climb condition,  $\alpha_C = 10^\circ$ ,  $\delta_p = \delta_a = \delta_r = \delta_e = 0$ ,  $i_f = -0.9^\circ$ ,  $T_e = .45$ , landing gear retracted,  $q = 16.37 \text{ lbs/ft}^2$ .

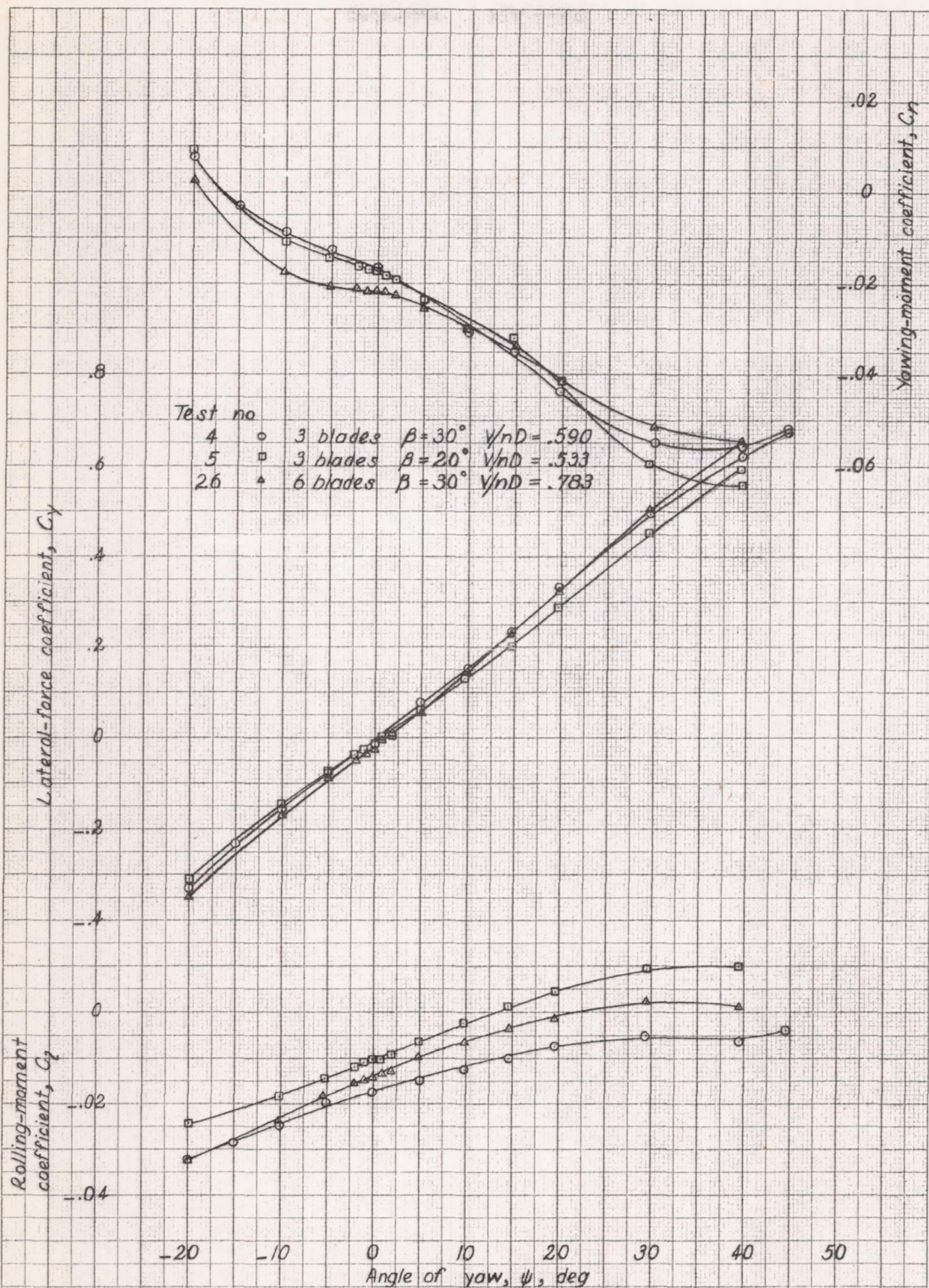


Figure 5 (continued).—Effect of propeller blade angle and number of blades on the aerodynamic characteristics in yaw of the 1/8 scale model of the Brewster F2A airplane. Approximately rated power. Climb condition,  $\alpha_c = 10^\circ$ ,  $\delta_p = \delta_a = \delta_r = \delta_e = 0$ ,  $i_p = -0.9$ ,  $T_c = 4.5$ , landing gear retracted,  $q = 16.37$  lbs/ft<sup>2</sup>.

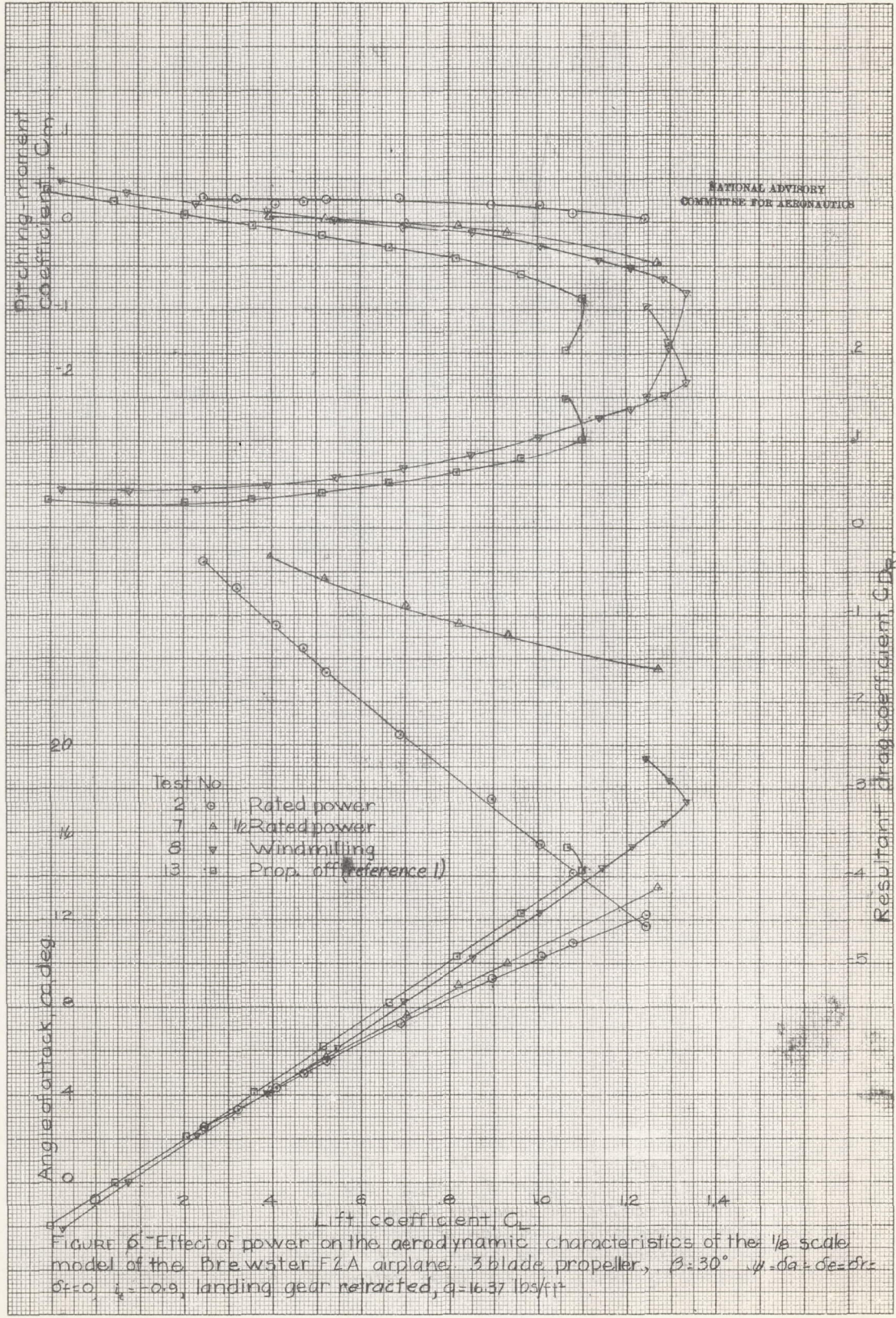


FIGURE 6—Effect of power on the aerodynamic characteristics of the 1/8 scale model of the Brewster F2A airplane, 3 blade propeller,  $\beta=30^\circ$ ,  $\psi=0$ ,  $\delta_a=\delta_e=\delta_r=\delta_f=0$ ,  $\delta_g=-0.9$ , landing gear retracted,  $q=16.37$  lbs/ft<sup>2</sup>

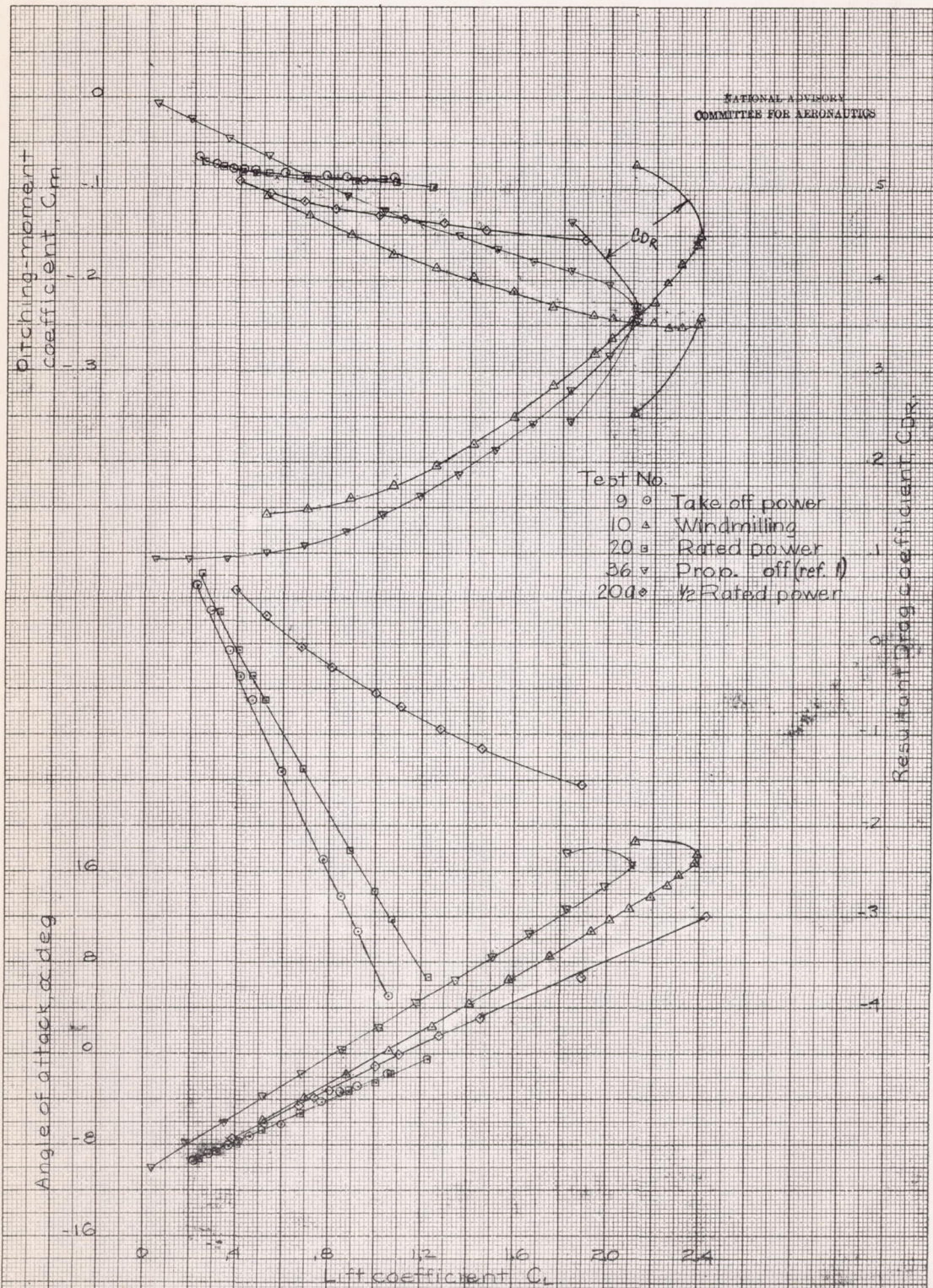


FIGURE 7. Effect of power on the aerodynamic characteristics of the  $\frac{1}{8}$  scale model of the Brewster F2A airplane. 3-blade propeller,  $\beta = 30^\circ$ ,  $\psi = 80^\circ$ ,  $\delta_f = 0$ ,  $\delta_r = 40$ ,  $i_t = -0.9$ , landing gear extended,  $q = 16.37$  lbs/ft $^2$ .

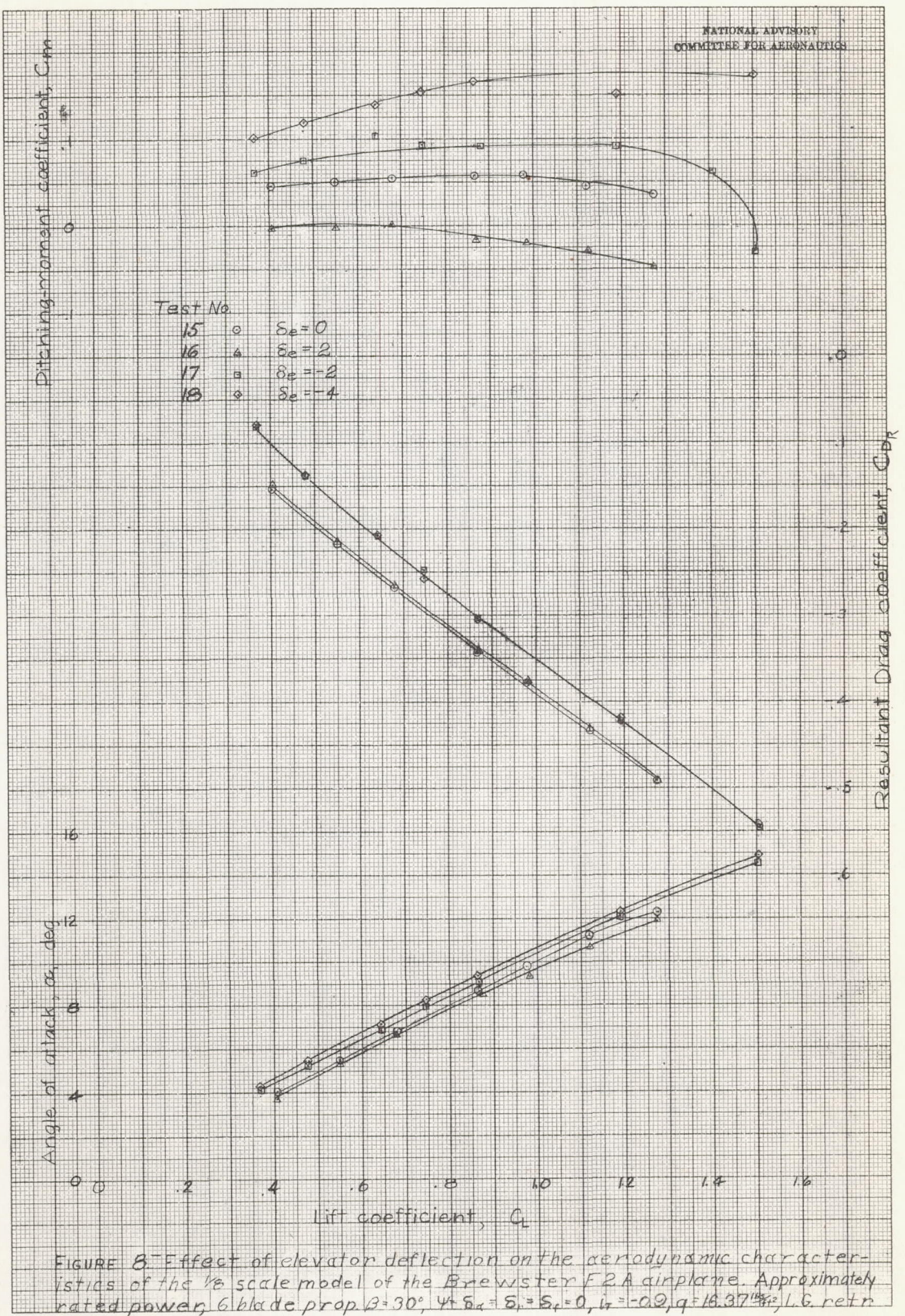


FIGURE 3—Effect of elevator deflection on the aerodynamic characteristics of the 1/8 scale model of the Brewster F2A airplane. Approximately rated power, 6 blade prop.  $\beta = 30^\circ$ ,  $\psi = \delta_a = \delta_r = \delta_f = 0$ ,  $\eta = -0.2$ ,  $q = 16.37 \text{ lb/ft}^2$ , 1.6 retr

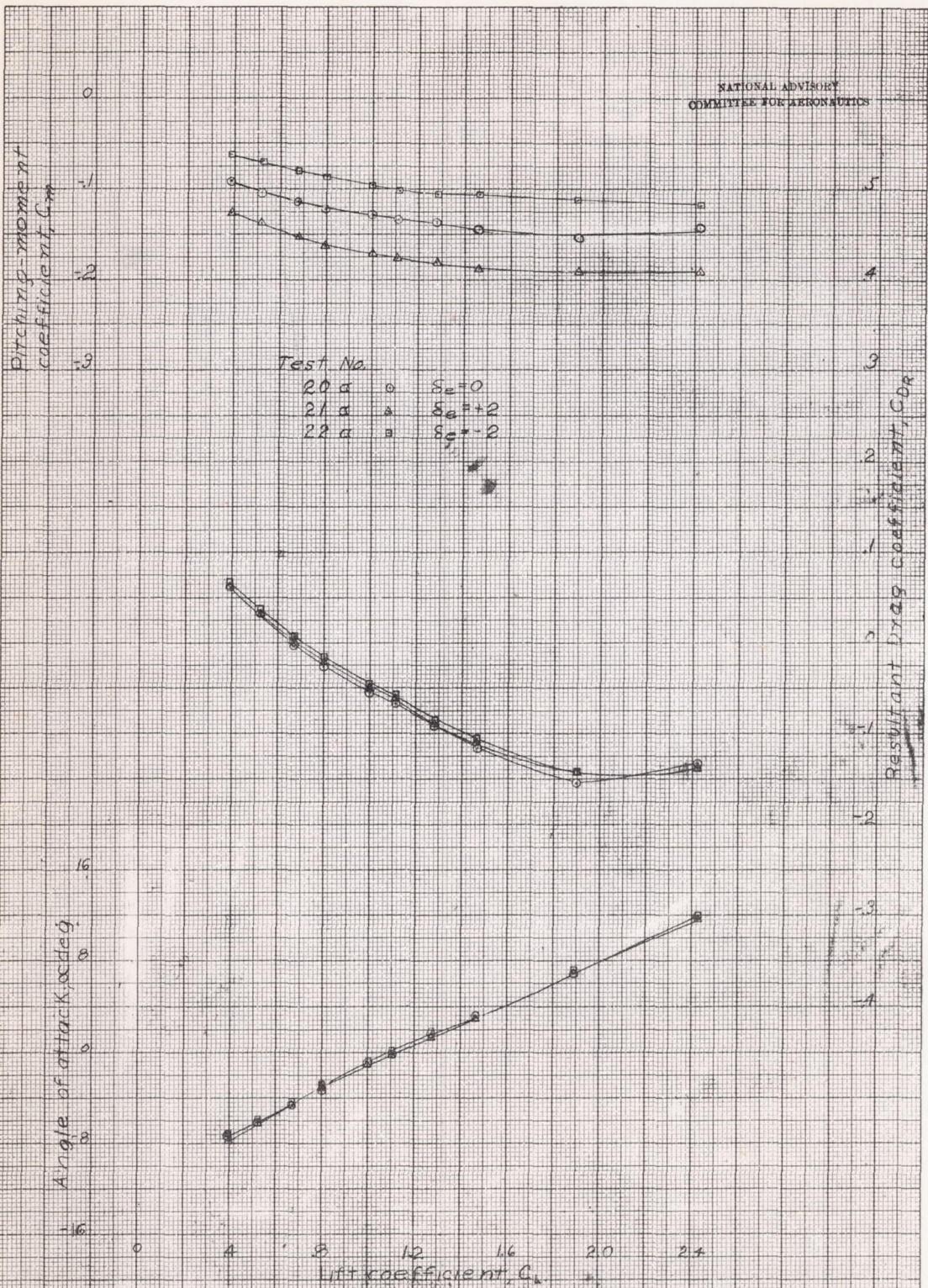
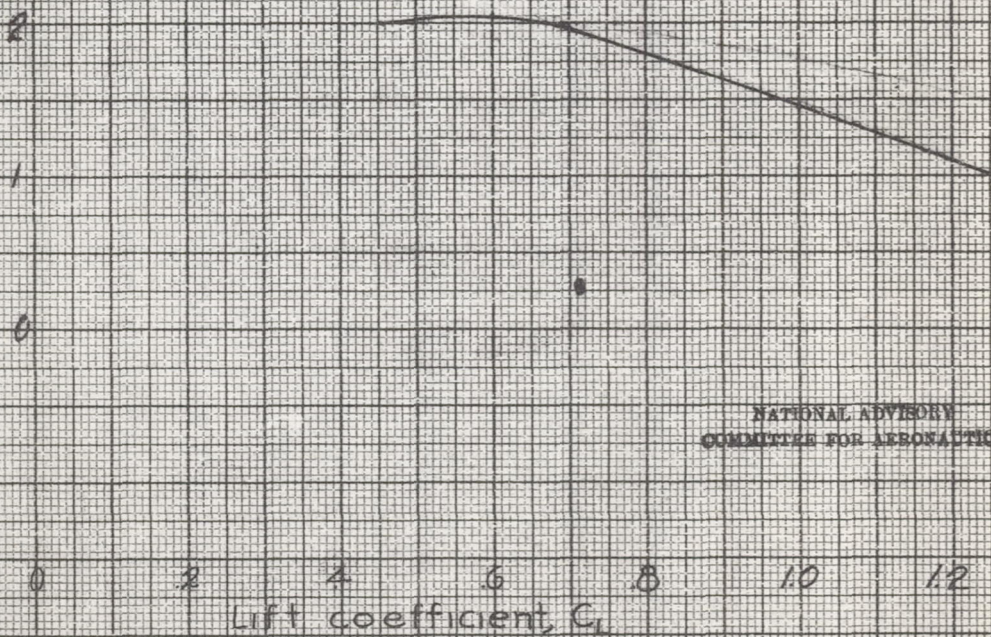


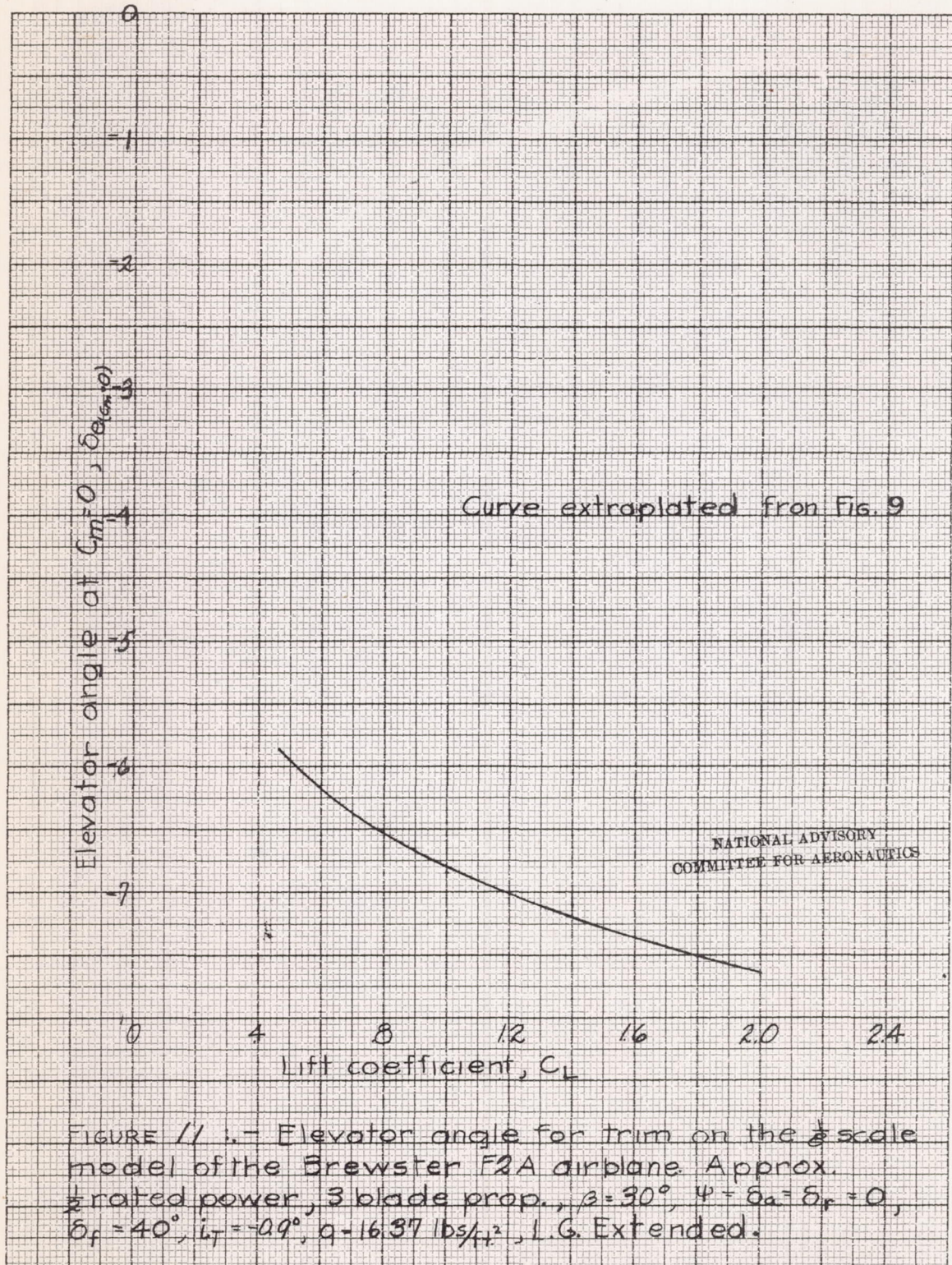
FIGURE 9.- Effect of elevator deflection on the aerodynamic characteristics of the 1/4 scale model of the Brewster F2A airplane. Approximately brated power, 3 blade propeller,  $\beta = 30^\circ$ ,  $\psi = 54^\circ$ ,  $\delta_e = 0$ ,  $\delta_r = 40$ ,  $\delta_l = -29$ ,  $q = 16.37 \text{ lb/ft}^2$ , L.G. extended.

Elevator angle for  $C_{m \cdot 0}$ ,  $\delta_{e(100-g)}$



NATIONAL ADVISORY  
COMMITTEE FOR AERONAUTICS

FIGURE 10 - Elevator angle for trim on the 3/8 scale model of the Brewster F2A airplane. Approx. rated power, 6 blade prop.,  $\beta = 30^\circ$ ,  $\psi = \delta_a = \delta_r = \delta_f = 0$ ,  $u_T = -0.9$ ,  $q = 16.37 \text{ lbs/ft}^2$ , L.G. retracted.



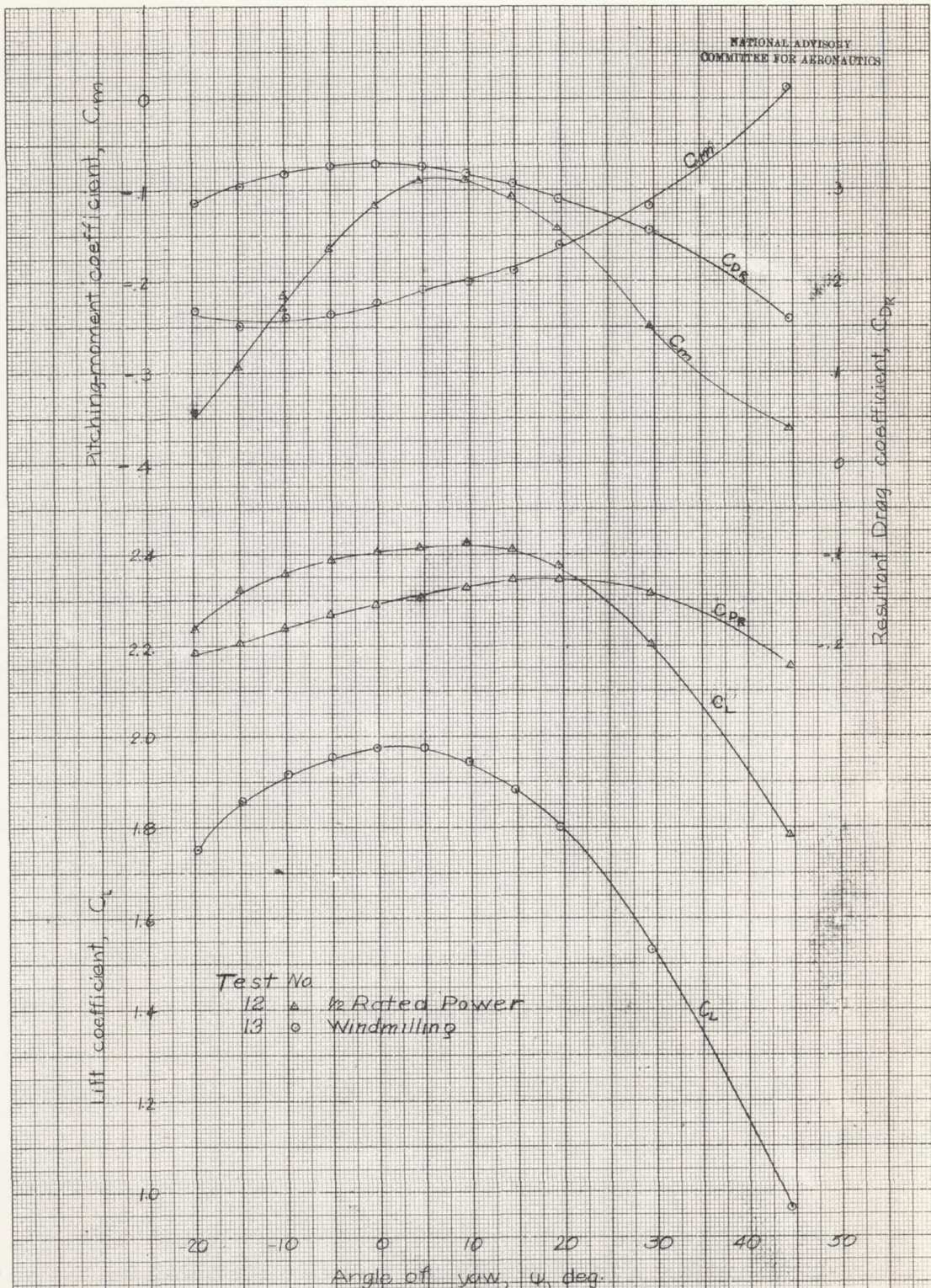


FIGURE 12.- Effect of power on the aerodynamic characteristics in yaw, of the 1/3 scale model of the Brewster F2A airplane. 3 blade propeller,  $\beta=30^\circ$  a. 11.2,  $T_c=0.570$ ,  $V_{ND}=0.535$ ,  $\delta_a=\delta_e=\delta_r=0$ ,  $\delta_s=4.0$ ,  $\delta_r=10.9$ , landing gear extended,  $q=16.3716/s^2$

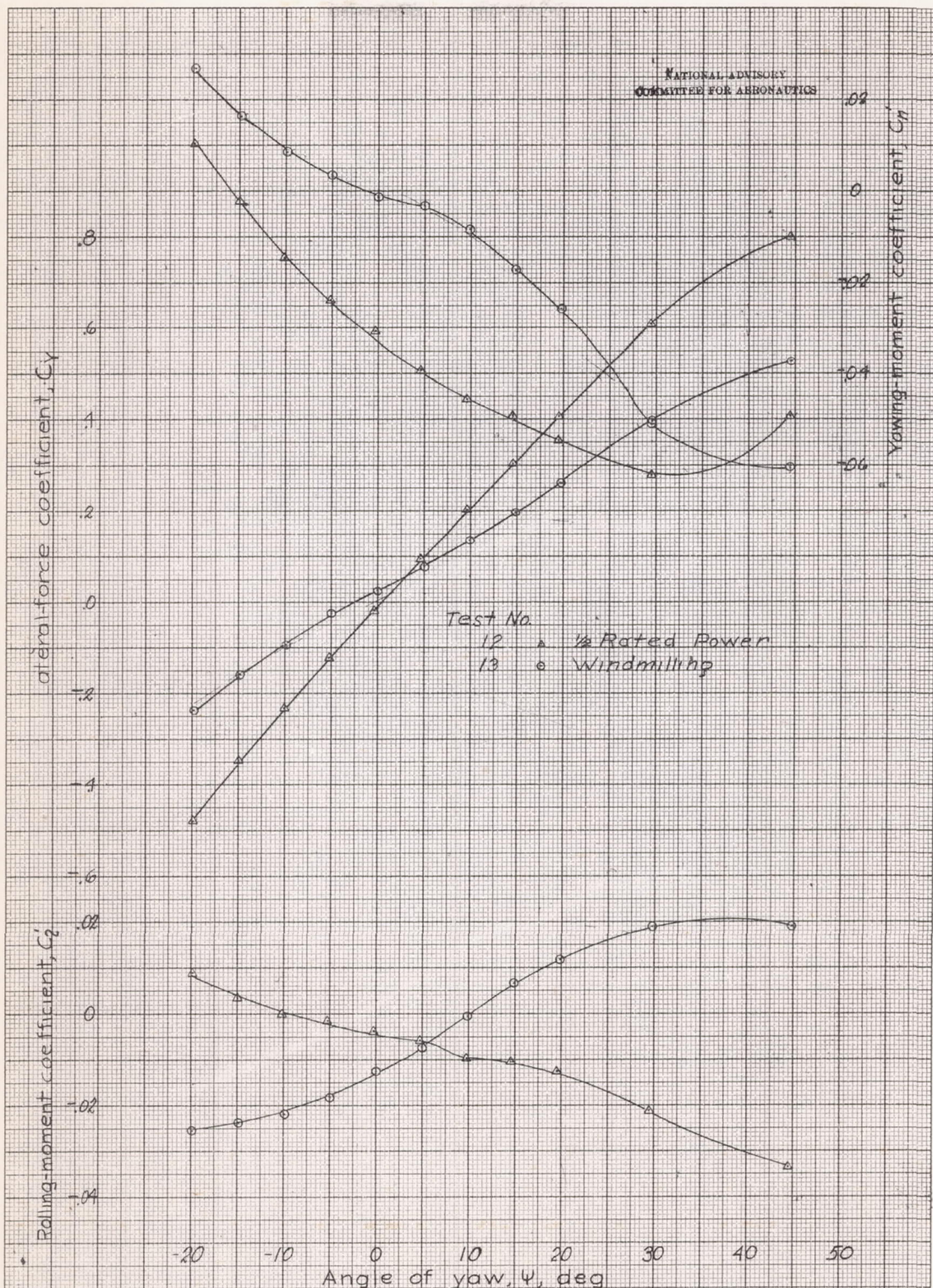


FIGURE 12-(Continued) Effect of power on the aerodynamic characteristics in yaw, of the 1/8 scale model of the Brewster F2A airplane. 3 blade propeller,  $\beta=30^\circ$ ,  $\alpha=11.2$ ,  $t_c=570$ ,  $V_{ND}=.535$ ,  $S_a=S_e=S_r=0$ ,  $S_f=40$ ,  $\zeta_f=+0.9$ , landing gear extended,  $q=16.37^{165/41.2}$

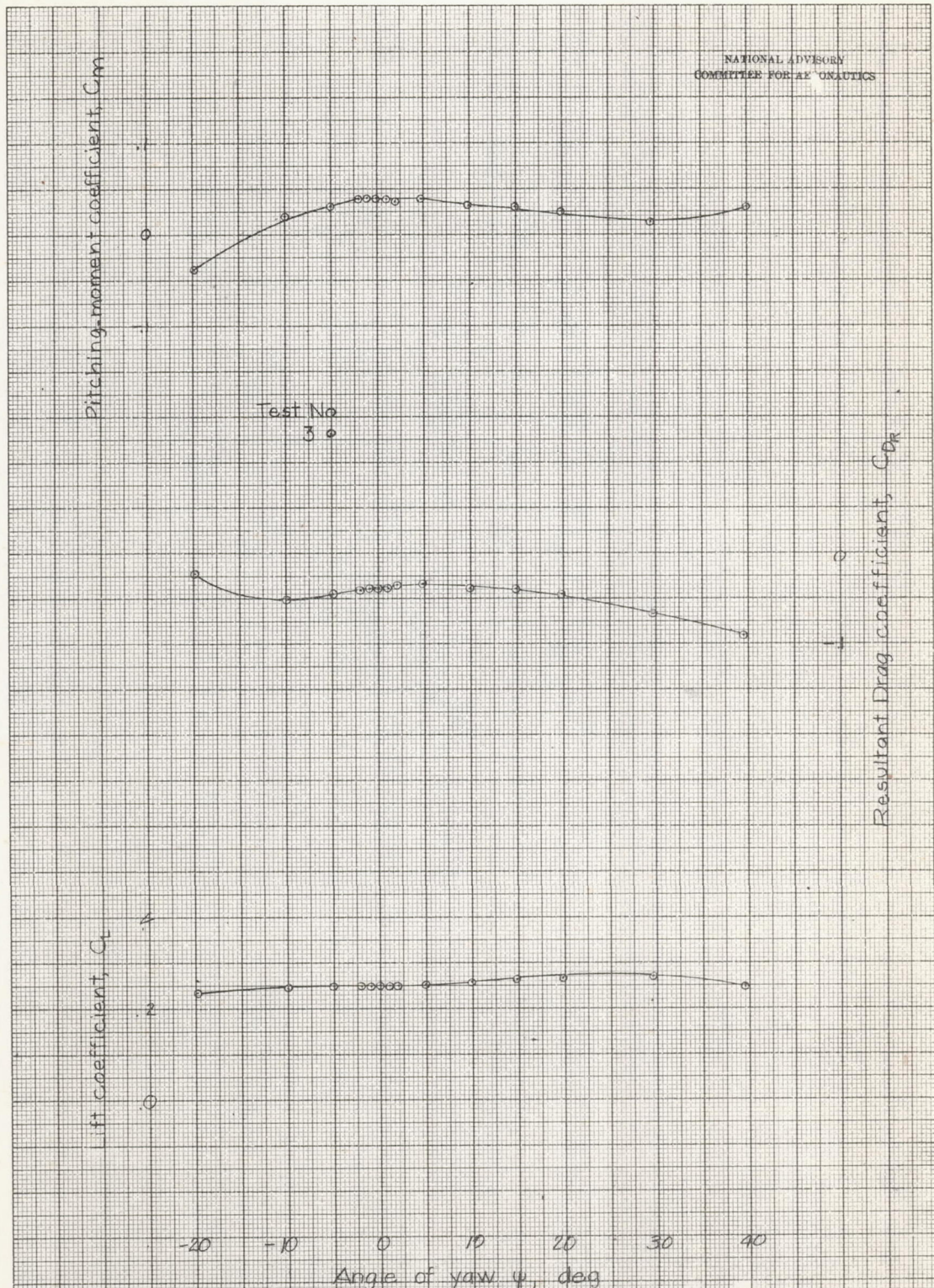


FIGURE 15—Aerodynamic characteristics in yaw of the  $1/8$  scale model of the Brewster F2A airplane. Approximately rated power, 3 blade propeller;  $\beta=30^\circ$ , high speed condition,  $\alpha=2.53$ ,  $T_C=.074$ ,  $V_{ND}=1.186$ ,  $\delta_e=\delta_r=\delta_f=0$ ,  $\delta_a=0$ ,  $i_L=-0.9$ , landing gear retracted,  $q=16.37$  lbs/ft<sup>2</sup>.

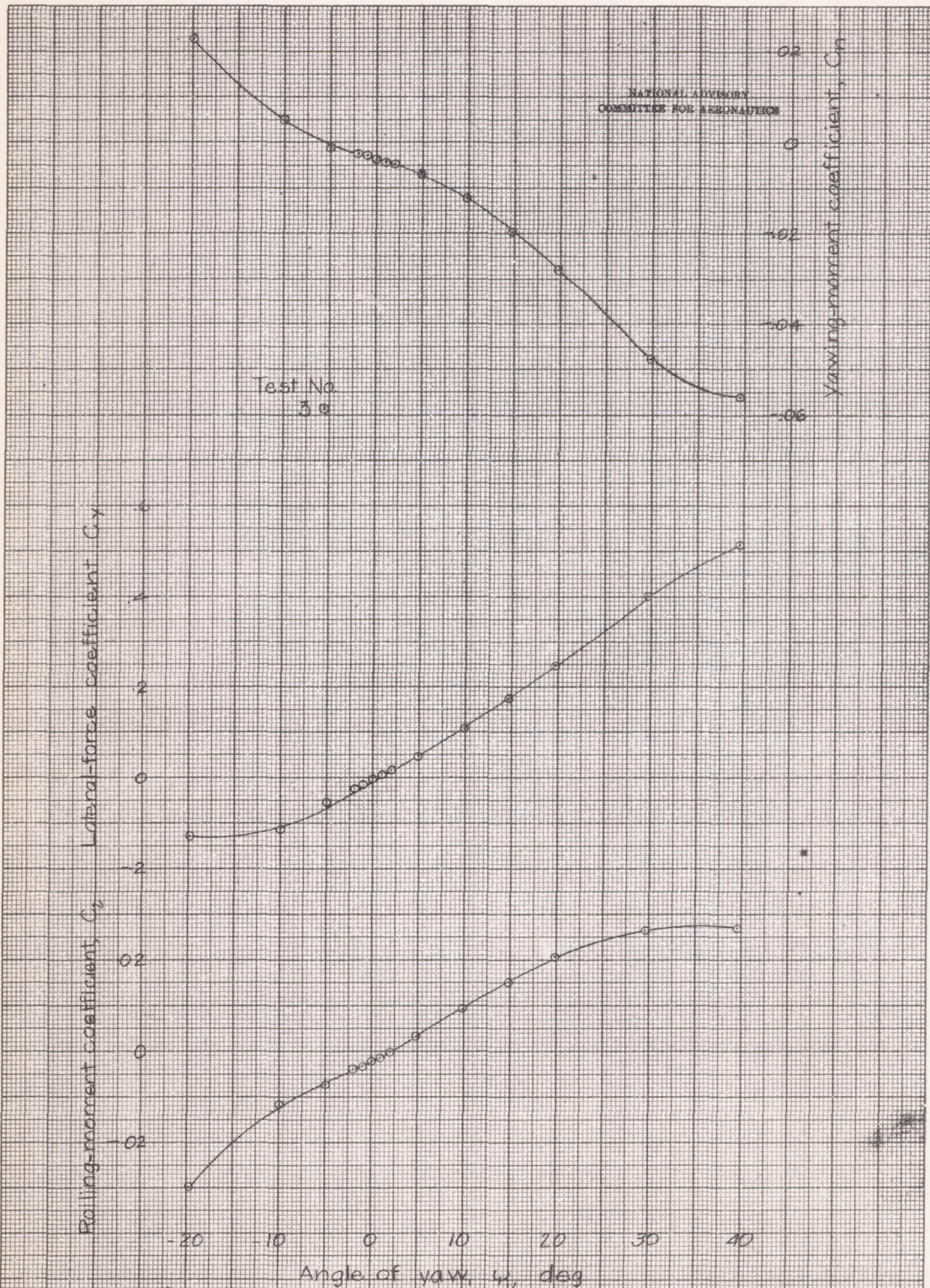


FIGURE 3 (continued) Aerodynamic characteristics in yaw of the 1/6 scale model of Brewster F2A airplane. Approximately rated power, 3 blade propeller  $\beta=30^\circ$ , high speed condition,  $\alpha=2.53$ ,  $T_c=0.74$ ,  $V/\Delta D=106$ ,  $q_c=0.0$ ,  $i_c=0$ ,  $i_c=-0.9$ , landing gear retracted,  $q=16.37$  lbs/ft<sup>2</sup>.

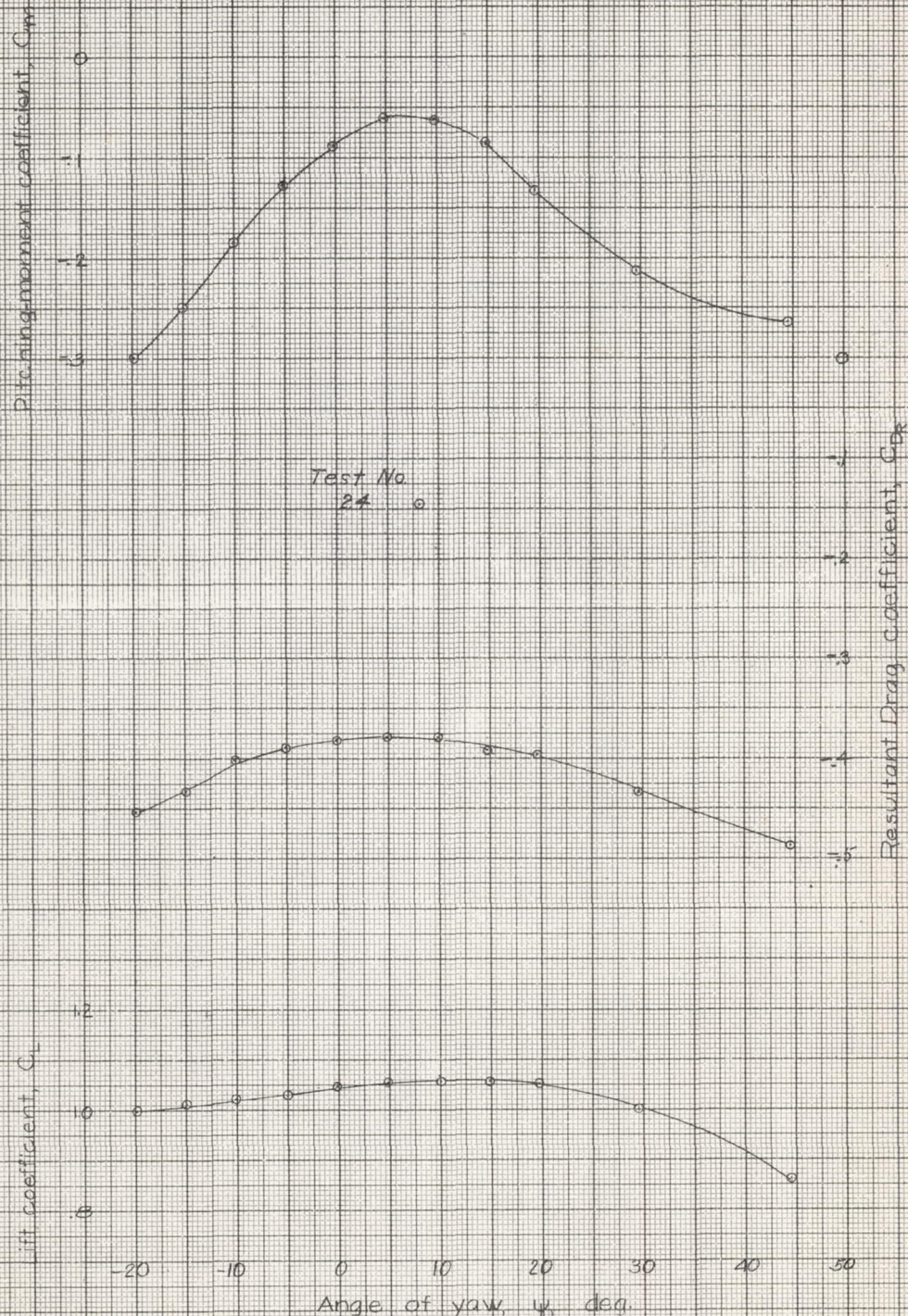


FIGURE 14 - Aerodynamic characteristics in yaw of the 1/4 scale model of the Brewster F2A airplane. Approximately take-off power, 3 blade propeller,  $\beta = 30^\circ$ ,  $\alpha = 1.76$ ,  $T_c = 5.70$ ,  $V_{ND} = 5.35$ ,  $S_c = 4.0$ ,  $S_e = S_d = S_f = 0$ ,  $l_r = -0.9$ , landing gear extended,  $q = 16.3716 \text{ lb/ft}^2$

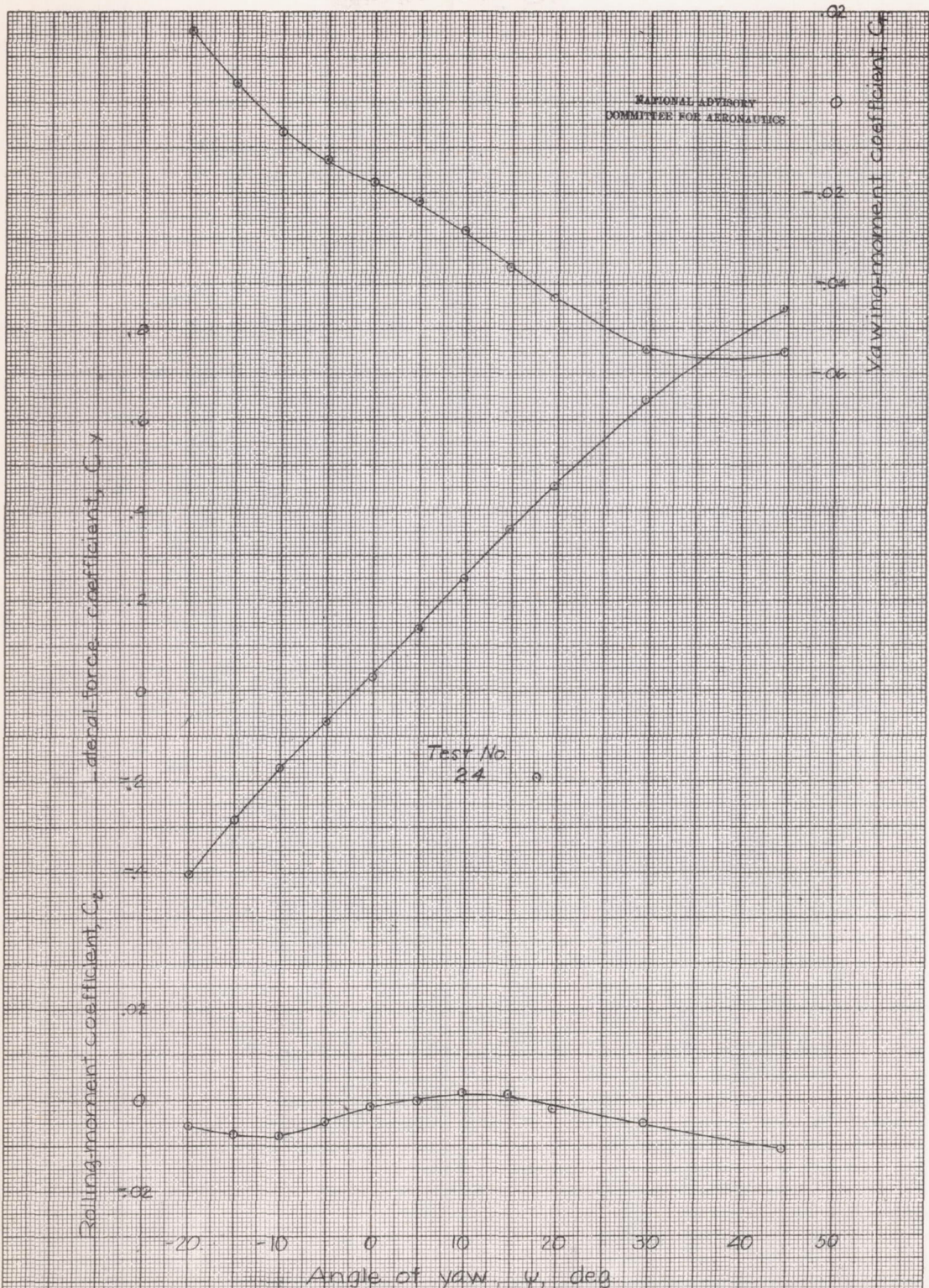


FIGURE 8 (Cont.)- Aerodynamic characteristics in yaw of the 1/8 scale model of the Brewster F2A airplane. Approximately take-off power, 3 blade propeller,  $\beta = 30^\circ$ ,  $\alpha = -1.76$ ,  $V = 570$ ,  $V_{ND} = 535$ ,  $\delta_e = \delta_a = \delta_r = 0$ ,  $i_T = -0.9$ , landing gear extended,  $q = 16.37$ ,  $\mu = 1.2$ ,  $\delta_T = 4.0$

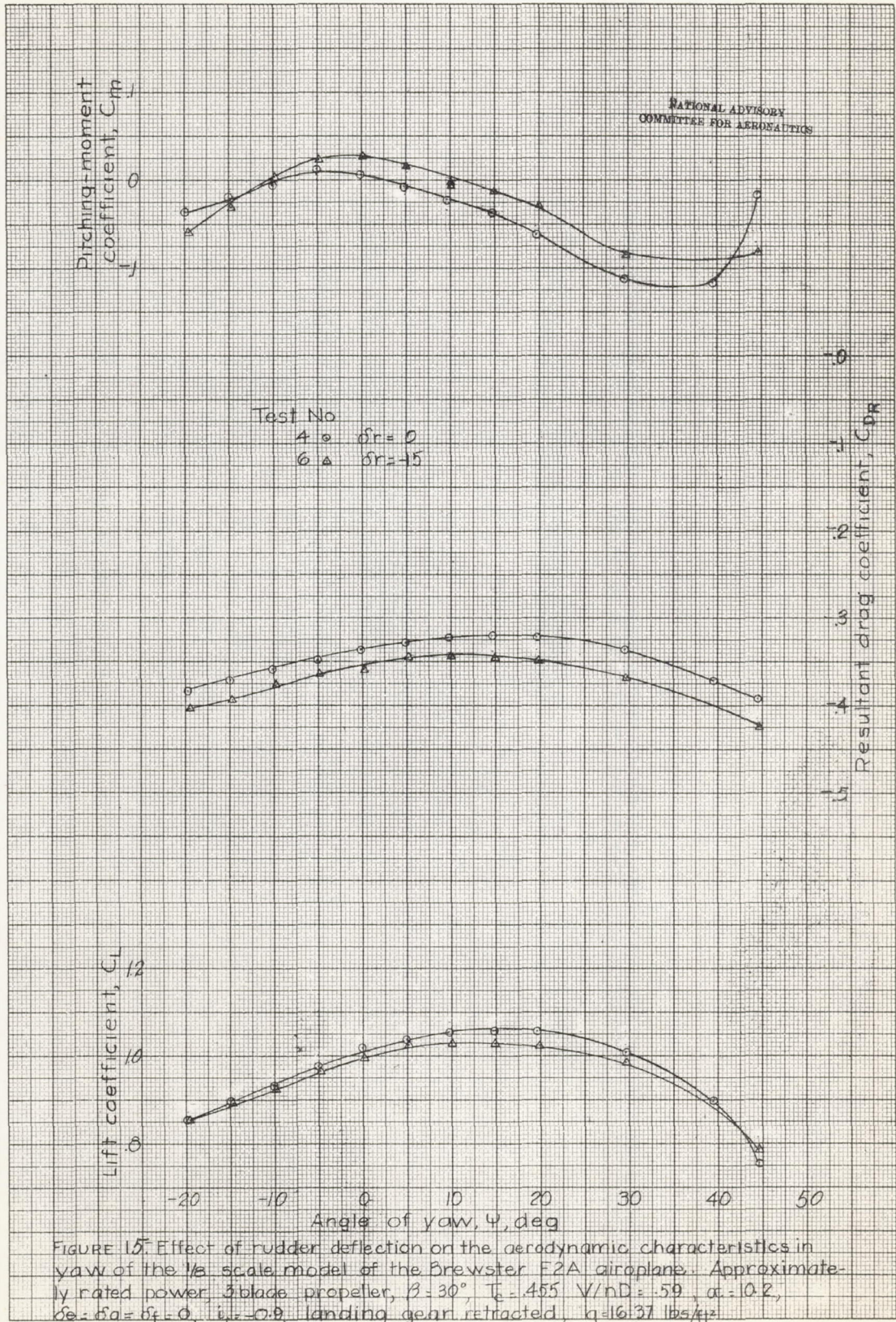
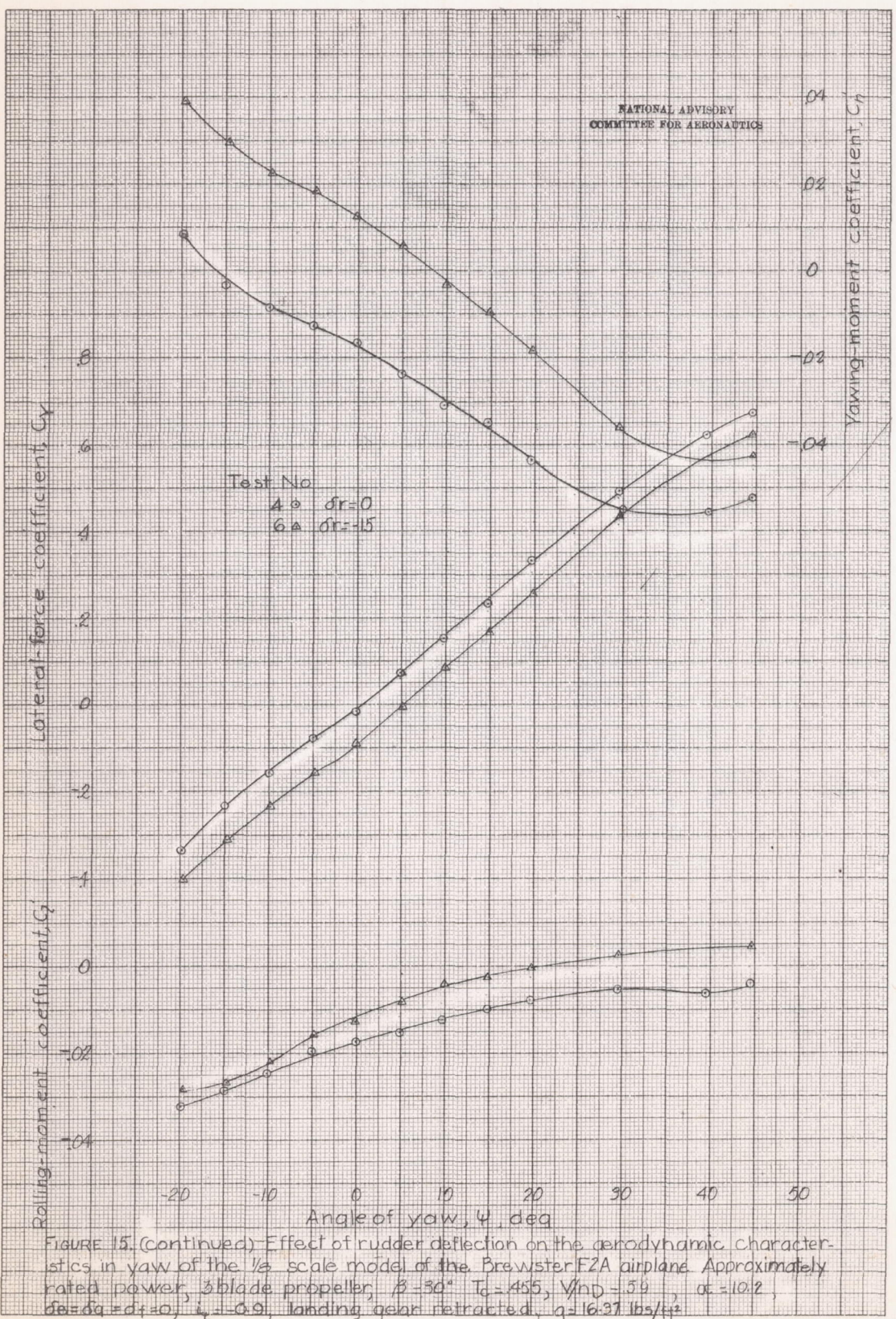


FIGURE 15. Effect of rudder deflection on the aerodynamic characteristics in yaw of the 1/8 scale model of the Brewster F2A airplane. Approximately rated power, 3 blade propeller,  $\beta = 30^\circ$ ,  $T_0 = 455$  V/nD = .59,  $\alpha = 10.2$ ,  $\delta a = \delta a' = \delta f = 0$ ,  $i_{L2} = -0.9$ , landing gear retracted,  $q = 16.37$  lbs/ft<sup>2</sup>.

L-707



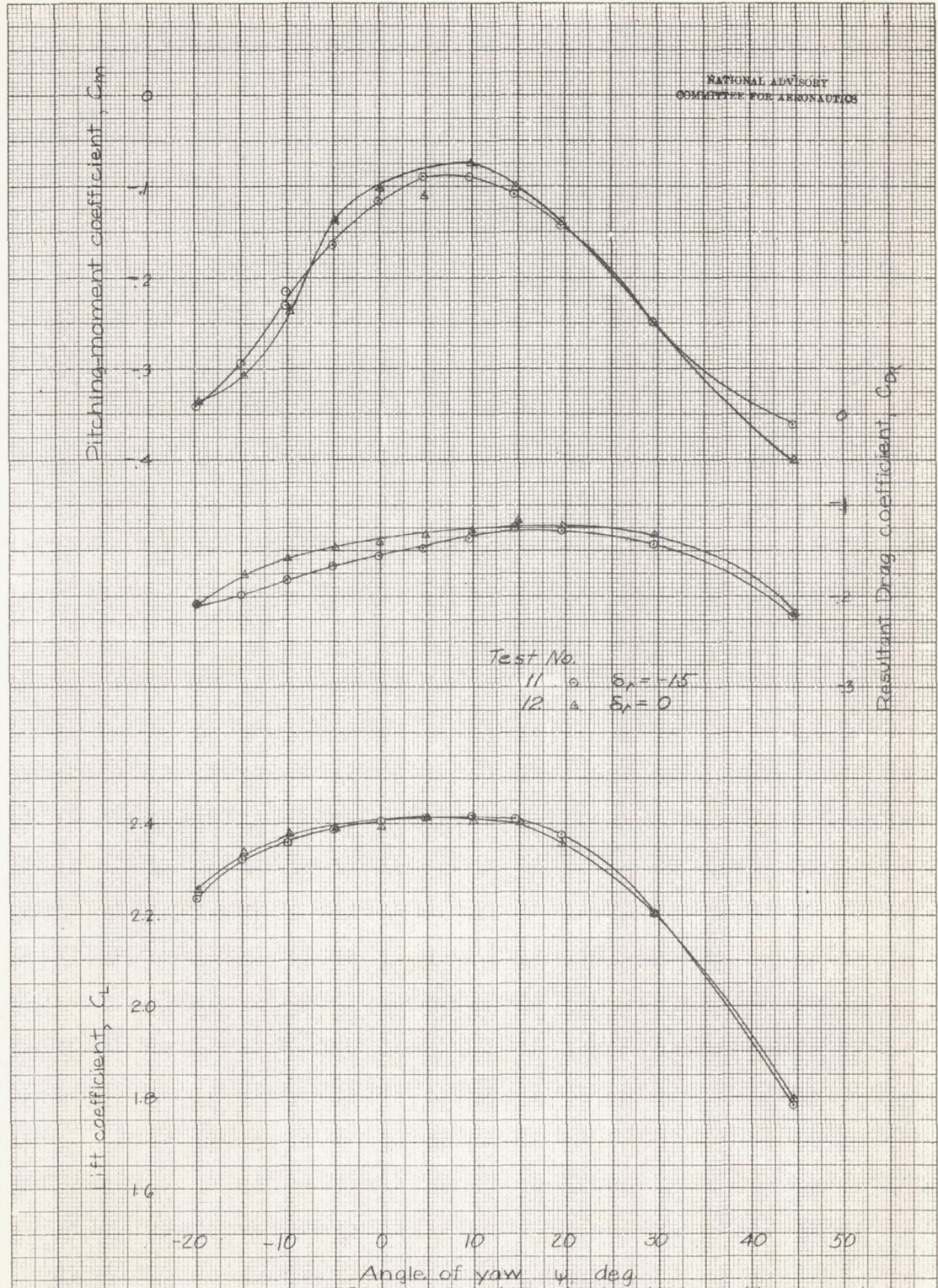


FIGURE 16.- Effect of rudder deflection on the aerodynamic characteristics in yaw of the  $V_8$  scale model of the Brewster F2A airplane. Approximately  $1/2$  rated power, 3 blade propeller,  $\beta = 30^\circ$ ,  $T_c = .570$ ,  $\gamma_{ind} = .535$ ,  $\alpha = 11.25^\circ$ ,  $\delta_e = \delta_d = 0^\circ$ ,  $\delta_r = 40^\circ$ ,  $\psi = -0.0$ ,  $q = 16.37 \text{ lbs./sq. ft.}$ , L.G. extended.

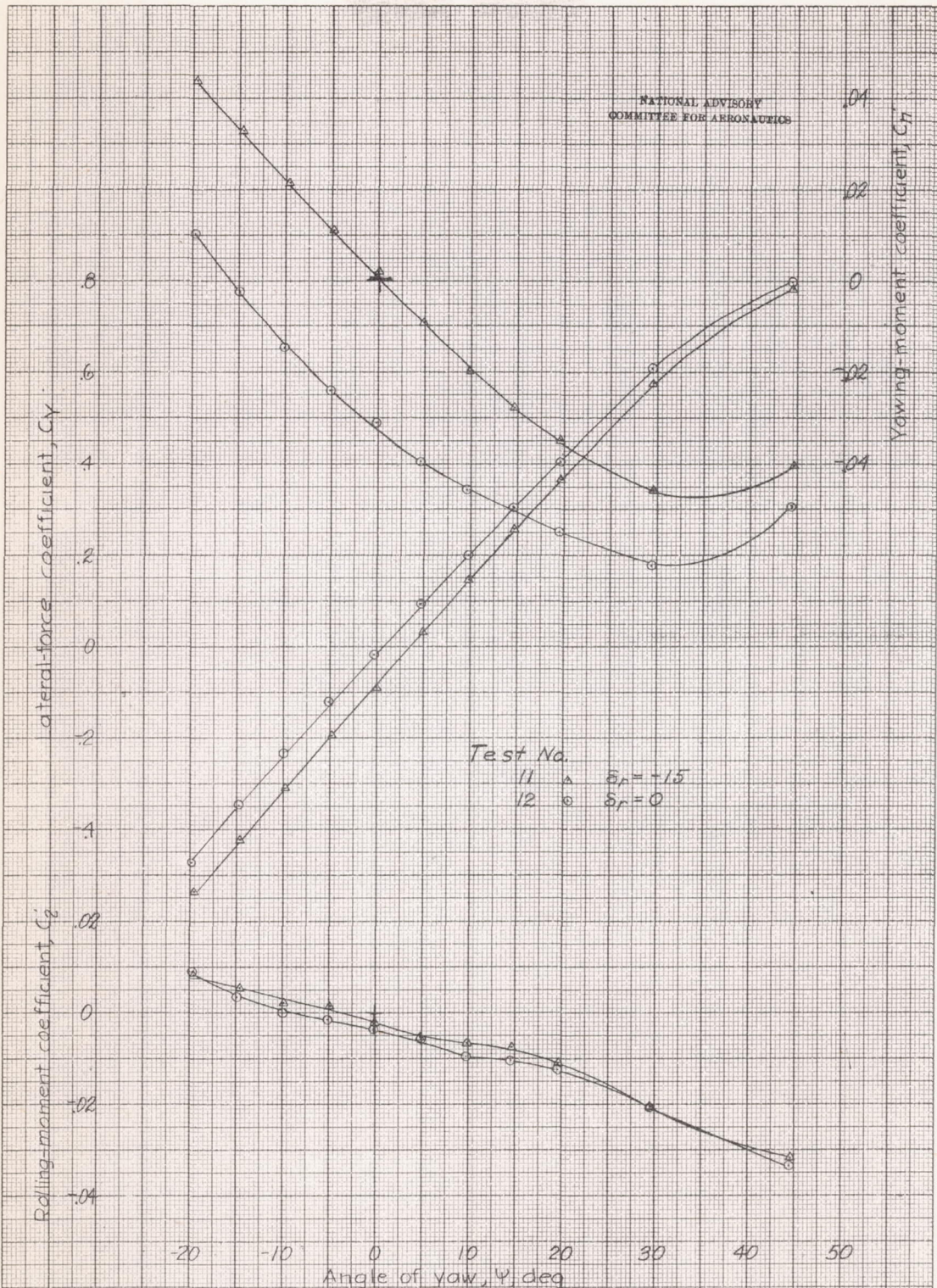


FIGURE 16 (Continued) Effect of rudder deflection on the aerodynamic characteristics in yaw of the  $1/8$  scale model of the Brewster F2A airplane. Approximately  $1/2$  rated power, 3 blade propeller,  $\beta = 30^\circ$ ,  $q = 16.37 \text{ lb/ft}^2$ ,  $T_c = 5.70$ ,  $V_{ind} = 53.5$ ,  $\alpha = 11.25^\circ$ ,  $\delta_e = \delta_a = 0$ ,  $\delta_r = 40$ ,  $\delta_f = -0.9$ , L.G. extended.

